Macula densa-dependent and non-macula densa-dependent signaling in the juxtaglomerular apparatus

PhD dissertation

Péter Komlósi, MD

Semmelweis University
Doctoral School of Basic Medicine

Mentor: **P. Darwin Bell, PhD**
Tutor: **László Rosivall, MD, PhD, DSc**
Program Leader: **László Rosivall, MD, PhD, DSc**
Official Academic Reviewers: **Zoltán Molnár, Ph.D**
President of the Examining Committee: **Emil Monos, MD, PhD, DSc**
Examining Committee Members:
Hilda Tost, MD, PhD
István Kiss, MD, PhD

2008, Budapest

Table of contents

LIST OF ABBREVIATIONS **4**

INTRODUCTION **6**

PHYSIOLOGICAL IMPLICATIONS OF THE JUXTAGLOMERULAR APPARATUS 6

EPITHELIAL SENSOR MECHANISMS 8

Apical components *8*

Basolateral components *10*

INTEGRATION/PROCESSING OF EPITHELIAL SENSORY INPUT 10

Macula densa intracellular signaling *10*

Modulation of macula densa cell sensing *12*

EPITHELIAL EFFECTOR/MEDIATOR SYSTEMS 12

Release of ATP *13*

Release of prostaglandin E_2 ..... *19*

Release of nitric oxide *21*

EVIDENCE FOR NON-MACULA DENSA-DEPENDENT TUBULE-TO-VASCULATURE CONNECTIONS 22

Juxtaglomerular connections *22*

OBJECTIVES **24**

METHODS **26**

ISOLATED PERFUSED PREPARATION 26

EXPERIMENTAL PROCEDURES 27

MULTIPHOTON FLUORESCENCE MICROSCOPY 28

WIDE-FIELD FLUORESCENCE MICROSCOPY 29

IMAGE ANALYSIS 30

STATISTICAL ANALYSES 30

RESULTS **31**

ASSESSMENT OF EPITHELIAL CELL VOLUME CHANGES 31

Effect of increases in $[NaCl]_L$ on MD cell volume as assessed by cytosolic dye concentration *31*
Effect of increases in $[NaCl]_L$ and osm_L on MD cell volume as assessed by cell membrane imaging *35*
Effect of $[urea]_L$ on MD cell volume *37*
ASSESSMENT OF EPITHELIAL INTRACELLULAR CALCIUM CONCENTRATION 39
Certain JGA elements demonstrate oscillations in $[Ca^{2+}]_i$ and V_{bl}. *40*
$[Ca^{2+}]_i$ signaling in perimacular cells is affected by the calcium-sensing receptor *44*
Flow and $[NaCl]_L$-dependent $[Ca^{2+}]_i$ signaling in the perimacular cells *45*
ROLE OF CELL VOLUME AND $[CA^{2+}]_I$ IN THE SIGNALING OF NO RELEASE AND VASCULAR RESPONSES..... 47
$[Ca^{2+}]_i$ dynamics during juxtaglomerular tubule-to-arteriole paracrine signaling *47*
DISCUSSION..... 49
CELL VOLUME STUDIES..... 49
INTRACELLULAR CALCIUM STUDIES 53
CONCLUSIONS..... 56
BIBLIOGRAPHY..... 58
BIBLIOGRAPHY OF THE CANDIDATE'S PUBLICATIONS 72
ACKNOWLEDGEMENTS..... 74
ABSTRACT 75
ABSTRACT IN HUNGARIAN (ÖSSZEFOGLALÁS) 76

List of abbreviations

$[Ca^{2+}]_i$	intracellular calcium concentration
$[Na]_L$	luminal sodium concentration
$[Na^+]_i$	intracellular sodium concentration
$[NaCl]_i$	intracellular sodium chloride concentration
$[NaCl]_L$	luminal sodium chloride concentration
AA	afferent arteriole
ADP	adenosine bisphosphate
AM	acetoxymethyl esther
AMP	adenosine monophosphate
AT_1 receptor	type 1 angiotensin II receptor
ATP	adenosine trisphosphate
cAMP	cyclic adenosine monophosphate
CFTR	cystic fibrosis transmembrane conductance regulator
COX-2	cyclooxygenase-2
cTAL	cortical thick ascending limb
$DiBAC_4(3)$	bis-(1,3-dibutylbarbituric acid) trimethine oxonol
DT	distal tubule
E-NPPase	ecto-nucleotide pyrophosphatases/phosphodiesterases
E-NTPDase	ecto-nucleoside trisphosphate diphosphohydrolases
ERK	extracellular signal-regulated kinase
G	glomerulus
GFR	glomerular filtration rate
HEPES	4-(2-hydroxyethyl)-1-piperazineethanesulfonic acid
IP_3	inositol trisphosphate
JGA	juxtaglomerular apparatus
MAPK	mitogen-activated protein kinase

MD	macula densa
mPGES	membrane-associated prostaglandin E_2 synthase
NaCl	sodium chloride
NHE	sodium hydrogen exchanger
NMDG	N-methyl-d-gluconate
nNOS	neuronal nitric oxide synthase
NO	nitric oxide
osm_L or OSM_L	luminal osmlolality
PGE_2	prostaglandin E_2
pS	pico Siemens
PSD	power spectrum density
RVD	regulatory volume decrease
SBFI	sodium binding fluorescence indicator
TAL	thick ascending limb
TGF	tubuloglomerular feedback
TMA-DPH	1-(4-trimethylammoniumphenyl)-6-phenyl- 1,3,5-hexatriene p-toluenesulfonate
TRP	transient receptor potential
TTYH protein	protein containing threonine-threonine-tyrosine-histidine motif
V_{bl}	basolateral membrane potential
VDAC	voltage-dependent anion channel
VSMC	vascular smooth muscle cell

Introduction

As first recognized by Golgi (26), the cortical thick ascending limb of the loop of Henle (cTAL) contacts the vascular pole of its parent glomerulus, creating a structural connection between tubules and vessels that has at least two functional consequences. Changes in fluid composition in the tubular segment produce changes in the vascular tone of the associated glomerular arterioles (a phenomenon known as tubuloglomerular feedback (TGF)) and alterations in the rate of renin release from granular cells (100). The tubular epithelial cells, along with the extraglomerular mesangial cells, the afferent, efferent arterioles and the renin-containing granular cells are considered to be the principal elements of the juxtaglomerular apparatus (JGA). At the site of direct contact with the glomerular hilus, the tubular cells present with a unique array of morphological characteristics (including condensation of nuclei and the presence of wide lateral intercellular spaces) and are called macula densa (MD) cells. The tubular segment proximal and distal to MD, is generally referred to as cTAL and distal tubule (DT), respectively.

Physiological implications of the juxtaglomerular apparatus

In terms of functional significance, the juxtaglomerular apparatus has been suggested to play a pivotal role in the regulation of renal hemodynamics. One fascinating feature of the renal blood flow is it striking capacity to maintain a relatively constant value in spite of varying systemic blood pressure, a phenomenon referred to as autoregulation of renal blood flow. One component of the machinery responsible for this is the myogenic mechanism, a seemingly autonomous feature of certain vascular beds to reactively constrict in response to increased perfusion pressure. The other component of the autoregulation is thought to be the tubuloglomerular feedback system, which is a multi-component signaling array involving the juxtaglomerular apparatus (Figure 1). Upon an incidental rise in glomerular filtration rate, the delivery of sodium chloride to the thick ascending limb of the loop of Henle is elevated. Although the reabsorption of sodium chloride at this segment is load-dependent, this compensatory increase in reabsorption is not complete; therefore the net result is an elevation in tubular fluid sodium chloride concentration. This is thought to be sensed by the macula

densa cells, which then release a mediator that leads to a compensatory constriction of the adjacent afferent arteriole, returning the glomerular filtration rate and renal plasma flow toward normal/baseline value.

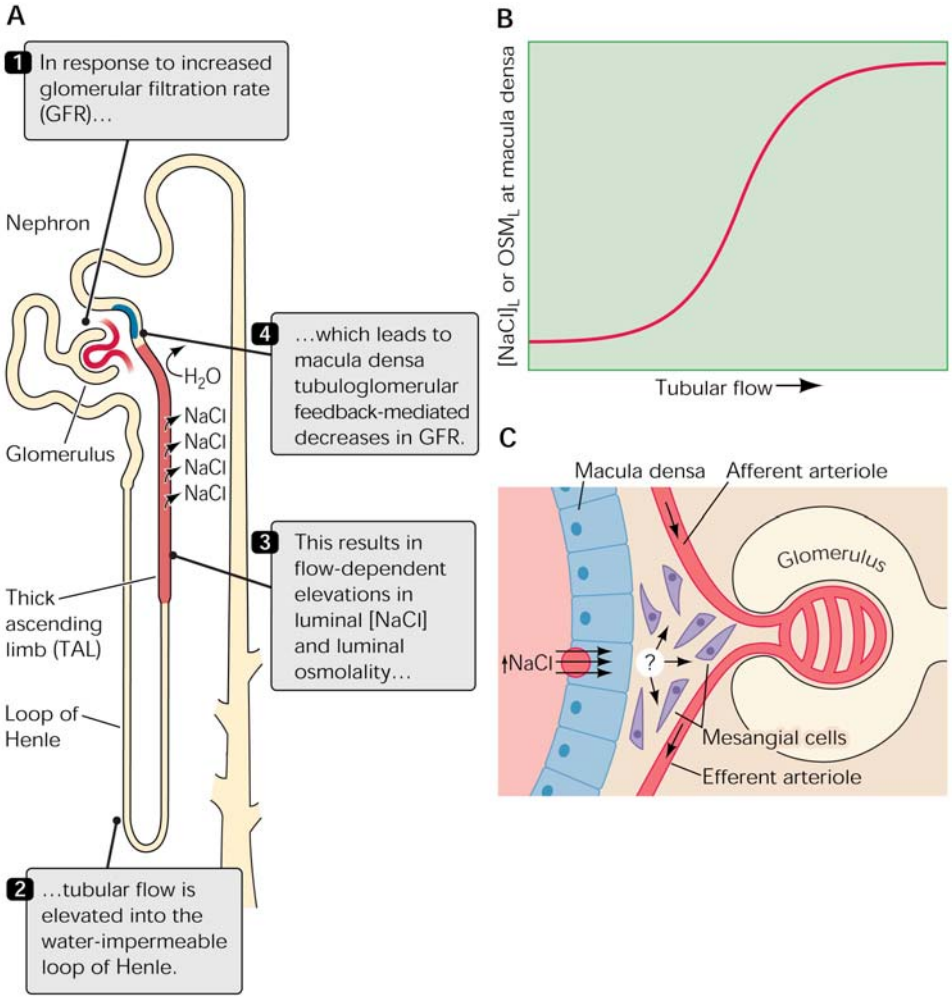

Figure 1 *A*: schematic diagram of a nephron. *B*: increases in flow rate increase luminal NaCl concentration ($[NaCl]_L$) and luminal osmolality (osm_L). *C*: relationship of the macula densa, mesangial cells, and afferent arteriolar smooth muscle cells. The nature of the chemical mediator that is released by the macula densa cells and that transmits information to the other components in this pathway remains unknown.

Another important function of the juxtaglomerular apparatus is the regulated release of renin from the granular cells of the afferent arteriole. Renin is the rate-limiting enzyme in the activation of the renin-angiotensin-aldosterone system, which is an important homeostatic mechanism aimed at maintaining a constant effective circulating volume.

Specifically, the release of renin from the juxtaglomerular apparatus cleaves angiotensinogen to give rise to angiotensin I which is further processed by angiotensin-converting enzyme to angiotensin II. Angiotensin II is a potent vasoactive substance and also one of the major stimulators of aldosterone production by the adrenal cortex. The release of renin is regulated primarily by three parameters: first, by the afferent arteriolar transmural pressure; second, by the renal sympathetic neural outflow via adrenergic receptors on the granular cells and third, by the sodium chloride delivery to the macula densa. It has been suggested that (especially under chronically salt-depleted conditions) acute decreases in tubular sodium chloride concentration lead to the release of a mediator (likely prostaglandin E_2) that then results in the release of renin from the granular cells.

Epithelial sensor mechanisms

Apical components

By virtue of their anatomical localization, MD cells have long been considered to be the primary sensor of changes in luminal fluid composition and signal-transducer that alters vascular resistance and controls the release of renin. Recently, a great deal of effort has been directed towards elucidating the ionic channels and carriers that are located at the apical and basolateral membrane of MD cells (Figure 2). At the apical membrane, the major NaCl entry pathway is the furosemide-sensitive $Na^+:K^+:2Cl^-$ cotransporter (NKCC2 or BSC1) that is responsible for ~ 80 % of apical NaCl entry into MD cells (59). MD cells appear to predominantly express the B isoform of NKCC2 (120) which has been shown to exhibit the highest affinity for chloride relative to the other isoforms. Thus, even at the lower limit of normal $[NaCl]_L$ (~ 15 to 25 mmol/L (98)) at the MD, the cotransporter still reabsorbs NaCl (59) while the cotransporter exhibits saturation and maximal transport rates at a $[NaCl]_L$ of 60 mmol/L (56).

The other apical pathway for sodium entry into MD cells is through the NHE2 isoform of the Na^+/H^+ exchanger; this transporter is responsible for ~ 20 % of apical Na^+ uptake into MD cells (22, 82). However, unlike with the $Na^+:K^+:2Cl^-$ cotransporter, Na^+/H^+ exchanger activity does not saturate as $[NaCl]_L$ is elevated above 60 mmol/L. In addition to influx of sodium, NHE's extrude hydrogen ions and so there is a $[NaCl]_L$-dependent cell alkalinization with a linear increase in cell pH at least over the range of

25 to 150 mmol/L $[NaCl]_L$. Therefore, the fact the Na^+:K^+:$2Cl^-$ cotransporter and Na^+/H^+ exchanger operate over different ranges in $[NaCl]_L$ provides the basis for suggesting that these two transport proteins may regulate separate paracrine signaling pathways.

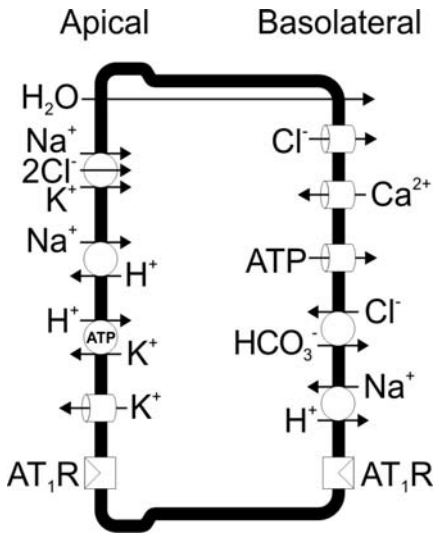

Figure 2 Overview of macula densa apical and basolateral membrane transport processes.

Unlike TAL cells, MD cells lack appreciable basolateral Na^+/K^+-ATPase activity, and it was suggested that they regulate intracellular sodium concentration $[Na^+]_i$ via an apically located, ouabain-sensitive colonic form of H^+/K^+-ATPase (79, 102). This transporter also extrudes Na^+, albeit less efficiently than the Na^+/K^+-ATPase. The absence of high-throughput Na^+ efflux systems should allow $[Na^+]_i$ to reflect luminal NaCl delivery to MD cells.

Using patch-clamp techniques, a high abundance of apical K^+ channels was detected in MD cells (42). Since the cotransporter and H^+/K^+-ATPase activities constitute a significant K^+ load into MD cells, a high-activity K^+ efflux pathway is required for sustainable coupling of apical Na^+ and K^+ transport. ROMK, a cloned K^+ channel, has been identified immunologically in TAL and macula densa (119) and may be responsible for all or part of apical K^+ secretion. In addition to K^+ recycling, this K^+ channel may be responsible for hyperpolarization and regulation of MD cell membrane potential. In particular, it may function in the cell hyperpolarization observed when $[NaCl]_L$ is reduced from high to low levels. Besides a K^+ channel, no other ionic conductances have yet been detected at the apical membrane of MD cells. However, there may be other transporters in this membrane and it is clear that some isoform of the

aquaporin water channel is also present in this membrane. The high water permeability at the macula densa segment may provide a path for a "trans-tissue" water flux though the fenestrated endothelium of the adjacent afferent arteriole (90, 91, 92).

Basolateral components

There is functional evidence suggesting the existence of a substantial basolateral chloride conductance in MD cells (57). This chloride permeability is proposed to be responsible for MD basolateral membrane depolarization in response to increased apical NaCl transport and increased intracellular chloride activity. Although the molecular identity of this channel has not been defined, preliminary patch-clamp studies indicate the presence of a ~ 20-pS anion channel at the basolateral membrane of MD cells. There is also a much larger anion conductive pathway (~ 350 to 400 pS) that is involved as an ATP conductive pathway.

A recent study has identified a non-selective, divalent cation-permeable channel in the basolateral membrane of MD cells (58). This ~ 20-pS channel is activated by membrane depolarization and elevations in $[Ca^{2+}]_i$. It exhibits a moderate Ca^{2+} permeability and biophysical characteristics that are very similar to members of the TRP family; members of this non-selective cation channel are known to be expressed in kidney. These cation channels may contribute to MD depolarization and elevation of $[Ca^{2+}]_i$ upon a rise in $[NaCl]_L$.

There is also evidence for conductive pathways for Na^+, K^+, and immunological and functional support for the existence of a Cl^-/HCO_3^- exchanger that may be involved in MD cell pH regulation (51). In addition, there is the NHE4 isoform of the sodium hydrogen exchanger (82) and indirect evidence for the existence of a sodium-calcium exchanger, all operating at the basolateral membrane. Thus the macula densa cells have a substantial repertoire of channels and transporters; the current challenge is attempting to understand the role of these various transport pathways in the MD cell signaling process.

Integration/processing of epithelial sensory input

Macula densa intracellular signaling

The large capacity for NaCl entry across the apical membrane coupled to the relatively weak Na^+ extrusion pathway, may result in MD $[NaCl]_i$ that reflects or tracks changes in $[NaCl]_L$ (4, 79, 95). This behavior would seem to be pivotal for the role of MD cells as sensors of tubular fluid flow and composition. Experimental work has verified that $[Na^+]_i$, measured with the fluorescent dye SBFI, parallels $[NaCl]_L$ over the range of 20 to 60 mmol/L. Although the consequence of sodium entry and increasing $[Na^+]_i$ are not completely known, it is clear that elevations in $[Na^+]_L$ drive the Na^+/H^+ exchanger resulting in MD cell alkalization.

NaCl influx also results in elevations in intracellular chloride concentration, which drives chloride ions through the basolateral chloride channels thereby depolarizing the basolateral membrane. One effect of basolateral membrane depolarization in MD cells is calcium entry, which may occur, in part, via the previously described non-selective cation channel (57, 81). Although previous work has reported that increases in $[NaCl]_L$ produce significant, but modest elevations in MD $[Ca^{2+}]_i$ (81) others have failed to find $[NaCl]_L$-dependent increases in MD $[Ca^{2+}]_i$ (97).

The finding that macula densa cells might be a water permeable "window" in the otherwise water impermeant cortical thick ascending limb (cTAL) was base of observations by Kirk *et al.* (48), using differential interference contrast microscopy. It was found that parallel increases in $[NaCl]_L$ and osm_L from 26 to 146 mmol/l and from 70 to 210 mOsm/kg H_2O, respectively, led to reversible decreases in macula densa cell height and narrowing of the lateral intercellular spaces. Also, transmission electron microscopic studies demonstrated closure of intercellular spaces between macula densa cells in cases where $[NaCl]_L$ and osm_L at the macula densa were expected to rise (47). According to both studies, changes in lateral intercellular spaces and cell height were specific to the macula densa cells and there were no changes in the surrounding cTAL. Studies by Gonzalez *et al.* (27, 28) also suggested that parallel increases in $[NaCl]_L$ and osm_L lead to decreases in macula densa cell height. Thus, these studies indicate that concordant elevations in $[NaCl]_L$ and osm_L lead to cell shrinkage due to a change in the osmotic gradient across the apical membrane.

In contrast, others reported $[NaCl]_L$ elevation-induced increases in macula densa cell volume, using fluorescence microscopy (63, 64). Also, a study from our laboratory concluded that elevations in $[NaCl]_L$ result in macula densa cell swelling (84).

However, these studies were performed by altering $[NaCl]_L$ while maintaining osm_L constant or minimally altered (84). Thus, there appears to be a conundrum regarding the effect of increasing $[NaCl]_L$ on macula densa cell volume.

In conclusion, there is a complex series of events that are involved in the sensing of tubular fluid flow and composition by MD Cells. Apical influx of NaCl resulting from increases in $[NaCl]_L$ results in elevations in $[NaCl]_i$, basolateral membrane depolarization, and increases in pH_i, $[Ca^{2+}]_i$ and cell volume. This cascade of events in MD cells results in the generation of paracrine signaling molecules but, what has become increasingly apparent, is that TGF responsiveness can be altered by controlling or modifying the sensitivity of these sensing mechanisms.

Modulation of macula densa cell sensing

Various hormones and alterations in physiological conditions can alter TGF responsiveness. One of the prime examples of TGF modulation is the vasoconstrictive hormone, angiotensin II. Previous studies have established that angiotensin II is an important and specific modulator of TGF (41, 67, 99, 104). Angiotensin II concentrations have been shown to be in the nanomolar range in renal tubular and interstitial fluid (72, 76). MD cells have also been shown to express AT_1 receptors on what appears to be both apical and basolateral surfaces (35). Recent work (116) has demonstrated that angiotensin II has a direct stimulatory effect on MD cells that may explain the effects of this hormone in TGF modulation. It was shown that low-dose angiotensin II added to either the apical or basolateral membranes increases not only sodium-hydrogen exchange activity (7, 80) but also enhances apical $Na^+:K^+:2Cl^-$ cotransport (54). These studies suggest that angiotensin II increases the sensitivity of the apical sensing step by enhancing the influx of NaCl across the luminal membrane for any given concentration of $[NaCl]_L$. This is only one example, of how TGF signal modulation can be controlled, there is no doubt, other hormones and agents can influence TGF signaling by altering the sensing function of the MD cells.

Epithelial effector/mediator systems

Once macula densa cells detected changes in the luminal environment signals are then sent through the mesangial cell field and on to the smooth muscle and granular

cells of the arteriolar elements. Although macula densa cells and the rest of the juxtaglomerular apparatus are in close proximity, there are no cell-to-cell junctions between macula densa and mesangial cells. Therefore, these cells are thought to communicate with other components of juxtaglomerular apparatus though the release of paracrine factors.

The advent of new fluorescent probes, the development of biosensor techniques capable of measuring the concentration of signaling molecules in the vicinity of cells, and their combination with classical *in vitro* microperfusion methods enabled the recent in-depth exploration of macula densa paracrine signaling (5, 53, 83).

Release of ATP

A little less than eighty years ago, Drury and Szent-Györgyi first reported the concept that purines act as extracellular signaling molecules (20). Over the intervening years, there has been the increasing awareness that extracellular adenyl purines, including ATP, have important and diverse effects on many biological processes. Critical to this signaling cascade is the presence of extracellular nucleotides. Although nucleotides can be released from injured cells or during cellular necrosis, there is increasing evidence for the regulated release or movement of nucleotides from cell to extracellular fluid. This can result in substantially elevated extracellular nucleotide concentrations within extracellular microdomains adjacent to the point at which the nucleotide is released. Considering the additional fact that extracellular nucleotides, including ATP, undergo rapid enzymatic degradation, it is apparent that the majority of the biological effects of extracellular nucleotides involves localized paracrine or autocrine signaling. Transduction of extracellular nucleotide signaling occurs through specific cell surface expression of nucleotide or purinergic receptors. Thus, ATP signaling involves three distinct steps: the first is release of ATP from the cell interior; second, is the extracellular regulation of ATP concentration via degradation; and third, is the binding of ATP to specific receptors.

ATP release: measured with the luciferin/luciferase bioluminescent assay, has been detected from a large number of different types of cells, including polarized epithelial cell lines (108). Several examples of stimuli that lead to the release of ATP

are extracellular hypotonicity (93), increases in intracellular calcium concentration ($[Ca^{2+}]_i$) (9) and elevated levels of cell cAMP (85). At the present time, ATP is thought to exit cells through either vesicular transport or channel-mediated release (94). Since ATP is almost exclusively present in its negatively charged form, plasmalemmal anion channels are tempting candidate mediators of extracellular ATP release. Several proteins for this ATP channel have been proposed including connexin hemichannels, the ATP-binding cassette transporters including the multi-drug resistance protein and CFTR (or associated proteins), a splice variant of the mitochondrial protein voltage-dependent anion channel (VDAC) (77) and the recently cloned TTYH group of proteins (107). At the present time, however, there is a lack of convincing data conclusively demonstrating that any of these candidate proteins serve as the sole or major pathway for the movement of ATP across the plasma membrane.

Extracellular ATP degradation: occurs through at least three different nucleotidases that are anchored to the outside of the cell membrane or secreted into interstitium fluid (123). Ecto-nucleoside trisphosphate diphosphohydrolases (E-NTPDases), are capable of the sequential removal of a phosphate from ATP and ADP. Ecto-nucleotide pyrophosphatases/phosphodiesterases (E-NPPases) also degrade ATP, giving rise to AMP and pyrophosphate. Ecto-5'-nucleotidase is the enzyme responsible for the final step in ATP degradation via removal of a phosphate group from AMP. It should be emphasized that both the release of ATP via channels and the presence of local degrading enzymes provide for a rapid local signaling process with fast on/off kinetics.

Purinergic receptors: that bind extracellular ATP are classified as P2 receptors to distinguish them from P1 receptors that are activated by adenosine. P2 receptors have been localized in almost all mammalian tissue. P2 receptors are subdivided into ionotropic P2X receptors and G-protein coupled P2Y receptor families (14). Activation of the more common P2Y receptors gives rise to IP_3-mediated Ca^{2+} mobilization while the P2X receptor is a non-selective cation channel that is permeable to Ca^{2+}. There are multiple members of both P2X and P2Y receptors and these individual isoforms differ in tissue distribution, affinity for nucleotides, and antagonists/agonist specificities. Recent studies suggest that various isoforms with the

P2X and P2Y families can also form multimeric complexes (73). For further information and details on purinergic receptors the reader is referred to the following review articles (60, 105, 113).

In kidney, P2X and P2Y receptors are expressed at both the apical and basolateral membranes of renal epithelial cells, in the renal vasculature, and glomerular mesangial cells and podocytes (111, 113). P2 receptor activation has been suggested to play a role in a number of renal processes including the regulation of renal hemodynamics, and tubular transport function.

Since there is a lack of specialized junctions or connections between macula densa cells and the adjacent mesangial cells, it has been presumed that a chemical mediator is responsible for the signaling that occurs between these two cell types; however, the nature of this mediator has remained elusive. The reason to consider ATP as a mediator of macula densa cell signaling was due, in part, to the elegant work of Inscho (43, 44, 45, 46) and also Navar *et al.* (66, 68, 74, 75) in defining the importance of P2 receptors in the control of the renal vasculature. Also, macula densa cells express low levels of basolateral Na^+/K^+-ATPase. Presumably these cells would have a high capacity to generate ATP and low energy utilization, at least in terms of transporting NaCl across the basolateral membrane. To further investigate ATP signaling by macula densa cells, a novel purinergic biosensor technique was employed. This involved using PC12 cells that express P2X receptors and either monitoring channel activity using patch-clamp or loading these cells with fura-2 and measuring $[Ca^{2+}]_i$. This biosensor cell was placed at the basolateral membrane of macula densa cells and ATP release was observed upon increases in luminal [NaCl] (5). It was found that the ATP release across the basolateral membrane of macula densa cells was consistent with its role in macula densa cell signaling. ATP release increased in proportion to luminal [NaCl], was inhibited by blocking salt transport by macula densa cells with furosemide, and that [NaCl]-dependent ATP release did not occur in cortical thick ascending limb cells. Also, the release of ATP was enhanced from macula densa preparations obtained from animals maintained on low-salt diet (52) which is consistent with the up-regulation of TGF that occurs during salt restriction. Thus, these studies demonstrate that there is a

local paracrine signaling process that involves ATP release across that basolateral membrane of macula densa cells.

What activates this ATP conductive pathway with elevations in luminal [NaCl] remains to be answered (Figure 3). Possible candidates are based on previous work in macula densa cells that found increases in [NaCl] cause elevations in macula densa intracellular concentrations of sodium (79), chloride (95, 97), calcium (81), basolateral membrane depolarization (3), changes in cell volume (27, 28, 64, 84) and intracellular alkalinization (22). The answer to this question remains an active area of research.

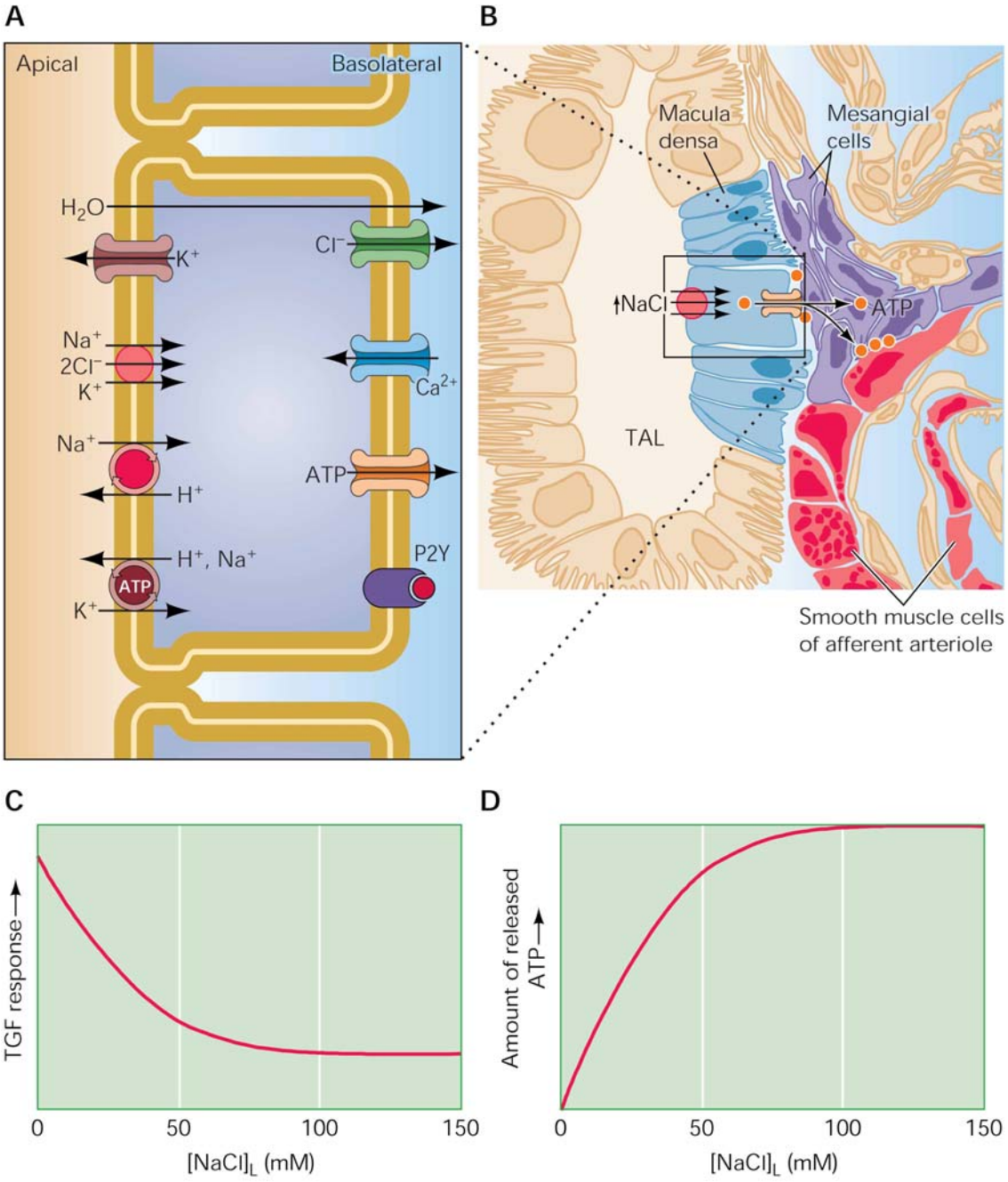
A
Apical
Basolateral
H_2O
K^+
Cl^-
Na^+
$2Cl^-$
K^+
Ca^{2+}
Na^+
H^+
ATP
H^+, Na^+
ATP
K^+
P2Y
B
Macula densa
Mesangial cells
NaCl
ATP
TAL
Smooth muscle cells of afferent arteriole
C
TGF response
0
50
100
150
$[NaCl]_L$ (mM)
D
Amount of released ATP
0
50
100
150
$[NaCl]_L$ (mM)

Figure 3 *A*: membrane transport events in macula densa cells that lead to the detection of changes in $[NaCl]_L$ and $[OSM]_L$ by these cells. *B*: an increase in $[NaCl]_L$ leads to an array of intracellular signaling events in the macula densa cells, which, in turn, increases basolateral maxi anion channel activity and the release of ATP into the cleft beneath the extraglomerular mesangial cells. ATP can then activate P2 receptors on the mesangial cells or on the vascular smooth muscle cells of the afferent arteriole. *C* and *D*: the relationship between TGF responses (downward curve representing decreases in GFR) and the associated increases in macula densa ATP that occur over the same range of $[NaCl]_L$.

Once released across the macula densa basolateral membrane, the exact role of extracellular ATP in signaling through the extraglomerular mesangial cell field and to the smooth muscle cells of the afferent arteriole is controversial. Mesangial cells and afferent arteriolar smooth muscle cells possess P2 receptors and this entire area of the juxtaglomerular apparatus contains abundant nucleotidases that would lead to the degradation of ATP. This would appear to be important since TGF signaling has relative fast kinetics (on the order of seconds) and thus would require rapid termination of ATP signaling. It is also possible that the rapid ATP degradation leads to the formation of adenosine and that subsequent P1 receptor activation plays a role in TGF signaling. Supporting this concept are studies by several groups showing that TGF responses are inhibited if A1 adenosine receptors or the adenosine-producing enzyme 5'-nucleotidase are pharmacologically blocked or genetically disrupted (11, 16, 103, 106, 109). What has not been entirely ruled out is the possibility that P1 receptor activity or integrity may play more of a permissive role in TGF signaling.

In this regard, Nishiyama *et al.* (74, 75) reported that renal interstitial concentration of ATP but not of adenosine parallels TGF-dependent adjustments in renal vascular resistance during changes in perfusion pressure. Also, interstitial infusion of ATP, probably via desensitizing P2 receptors, blocks TGF responses (68). In addition, as proposed by Inscho *et al.* (44), ATP-mediated activation of $P2X_1$ receptors is a prerequisite for TGF-dependent autoregulatory afferent arteriolar vasoconstriction. Therefore, ATP can readily diffuse to the smooth muscle cells of the afferent arteriole

and bind to $P2X_1$ and/or $P2Y_2$ receptors and thereby produce afferent arteriolar vasoconstriction (Figure 3).

ATP released across the basolateral membrane can cause increases in mesangial $[Ca^{2+}]_i$ via P2 receptor activation. This has clearly been shown in studies where cultured mesangial cells and not PC12 cells were used as biosensor cells in macula densa ATP-signaling experiments. Also, as reported by Gutierrez *et al.* (32), adenosine alone or P1 receptor activation does not lead to increases in mesangial $[Ca^{2+}]_i$. Since mesangial cells and the smooth muscle cells of the afferent arteriole are interconnected via gap junctions, it seems logical that one component of TGF signaling involves P2 receptor mediated signaling through the mesangial cell field and to the smooth muscle cells of the afferent arteriole. This paradigm is supported by the demonstration that abrogation of mesangial cells inhibits TGF responses *in vitro* (86). However, additional studies are needed to fully clarify the role of P1 and P2 purinergic receptors in macula densa-TGF signaling. In this regard, it has been reported that the distribution of ATP degrading enzymes closely correlates with the expression pattern of P2 receptors, suggesting that ATP degradation might be necessary for P2 receptor activation to happen (49). In other words, juxtaglomerular vascular function may depend on the concerted interplay of P1 and P2 purinergic activation.

Release of prostaglandin E_2

MD cells express the enzymes which synthesize prostaglandin E_2 (PGE_2) including cyclooxygenase-2 (COX-2) and the microsomal form of prostaglandin E_2 synthase (mPGES) (15, 23, 34). A recent study has provided direct evidence that MD cells synthesize and release PGE_2 at the basolateral membrane in response to reduced $[NaCl]_L$ (83). This study supported a previous observation (121) that decreases in ambient NaCl concentration led to PGE_2 release in a cell culture model that has been reported to be of macula densa cell origin. In the studies of Peti-Peterdi *et al*, the release of PGE_2 was restricted to changing $[NaCl]_L$ from ~ 80 to 0 mmol/L and only from animals that had been maintained on a low NaCl diet. This finding also correlated with the observation that COX-2 and mPGES are substantially up-regulated during dietary salt restriction. Although chloride transport-dependent activation of MAPK cascade members ERK and p38 has been reported in the putative cultured MD cells line

(121), the link between changes in $[NaCl]_L$ and increased MD PGE_2 release remains elusive (Figure 4).

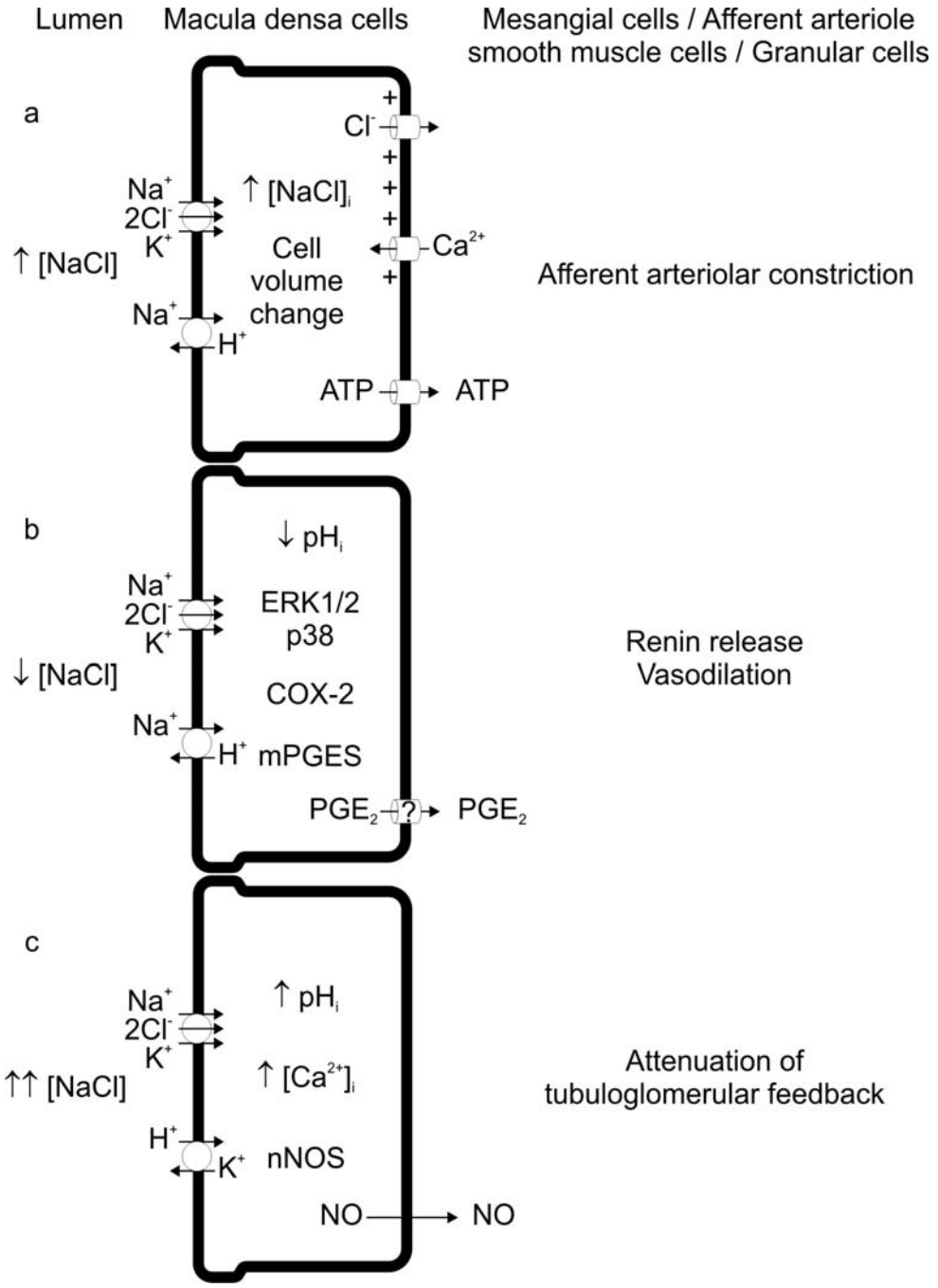

Figure 4 Models of macula densa signaling in response to different luminal NaCl concentrations. (a) An increase in $[NaCl]_L$ up to ~ 60 mmol/L leads to apical NaCl entry into macula densa cells primarily through the $Na^+:K^+:2Cl^-$ cotransporter and ATP release through basolateral maxi-anion channels, (b) a marked decrease in $[NaCl]_L$, especially under low dietary salt conditions, causes activation of the prostaglandin-synthesizing machinery, including cyxlooxygenase-2 (COX-2) and microsomal prostaglandin E_2 synthase (mPGES) and prostaglandin E_2 release across the basolateral membrane, which will be ready to promote the release of renin from granular cells, and (c) above a $[NaCl]_L$ ~ 60 mmol/L, macula densa cells pH will continue to increase via the apical Na^+/H^+ exchanger, which, will lead to nitric oxide production via activation of the neuronal isoform of nitric oxide synthase (nNOS).

Release of nitric oxide

Nitric oxide (NO), presumably released by MD cells, has been shown to attenuate TGF responses (117) and influence renin release from granular cells. This is based, to a large extent, on the high levels of neuronal-type nitric oxide synthase (nNOS) that have been immunologically detected in MD cells. Although TGF studies would suggest that increased $[NaCl]_L$ leads to NO production, a report, using NO sensitive electrodes, in fact found an inverse relationship between luminal NaCl delivery and distal tubular NO concentration (61, 101). Recently, with the development of NO-binding, high-sensitivity fluorescent dyes, a more direct way of addressing MD NO release became possible. It has been reported, that MD intracellular NO concentration increases with elevations in $[NaCl]_L$ (53, 64). This may suggest that the NO that was measured with microelectrodes could be due to NO generation by other cell types including the prior segments of the TAL. Also it has been found, that NO release was mostly stimulated by supraphysiological (above 60 mmol/L) $[NaCl]_L$. In this range of $[NaCl]_L$, the apical $Na^+:K^+:2Cl^-$ cotransporter is saturated, and changes in $[NaCl]_L$ are not reflected in changes in $[Na^+]_i$. However, $[NaCl]_L$ above ~ 60 mmol/L (22) further alkalinizes MD cells. Although nNOS is traditionally thought to be a calcium-sensitive enzyme, other work has reported that it is also pH sensitive (30). A

recent study suggested the possible involvement of changes in intracellular pH in the regulation of renin content in the granular cells (33). The tentative suggestion that the activity of the MD nNOS may be influenced by intracellular pH is supported by studies suggesting that the modulation of in vitro TGF responses via apical Na^+/H^+ exchanger may be NO dependent (115). However, additional work is needed to clarify the role of intracellular calcium and pH in the regulation of nNOS activity in MD cells. It should also be mentioned that this discussion is relevant to short-term regulation of MD NO production and there appears to be other mechanisms, for instance during alterations in dietary salt intake, that regulate the expression and perhaps activity of MD nNOS.

Evidence for non-macula densa-dependent tubule-to-vasculature connections

Juxtaglomerular connections

Interestingly, cells with morphologic features reminiscent of MD cells are found situated peripheral to the region of the MD in contact with the vascular component (2, 17, 29). The functional significance of these cells is unknown, but the observation that neuronal nitric oxide synthase (2) immunoreactivity is displayed not only by the MD cells but also by these "perimacular" cells located in the wall of the cTAL and DT might indicate functional similarities. In addition, as reported previously (1), and also as shown on Figure 13, there is an extensive region of contact between the distal tubule and the afferent arteriole.

By virtue of their anatomical localization, MD cells have long been considered to be the primary sensor of changes in luminal fluid composition and signal-transducer that alters vascular resistance and controls the release of renin. It was shown with *in vivo* micropuncture, that the small stop flow pressure (an index of glomerular capillary pressure, and therefore of vascular resistance) response to a hypotonic NaCl solution was restored to the full response by adding a Ca^{2+} ionophore to the retrograde perfusate, whereas the response to an isotonic NaCl solution was only marginally affected (6). To demonstrate the effect of the Ca^{2+} ionophore, the presence of Ca^{2+} in the perfusate was required. Luminal administration of a blocker of Ca^{2+} release from intracellular stores induced a dose-dependent reduction in the TGF response produced by an isotonic

electrolyte solution (8). Also, in the double-perfused JGA nephron preparation, reducing luminal Ca^{2+} concentration to zero caused afferent arteriolar vasodilatation (70).

A possible role for Ca^{2+} in the TGF response is supported by the observation that elevated $[NaCl]_L$ is associated with a modest but significant rise of $[Ca^{2+}]_i$ in MD cells (81). The rise in $[Ca^{2+}]_i$ was caused by cellular depolarization and opening of voltage-dependent Ca^{2+} channels in the basolateral membrane of MD cells. On the other hand, others failed to find $[NaCl]_L$-dependent increases in MD $[Ca^{2+}]_i$ (63, 96, 97). In other words, we have strong evidence for the role of intracellular Ca^{2+} in juxtaglomerular signaling, although the involvement of MD intracellular Ca^{2+} in this process is controversial. One possible explanation for this conundrum is that at least one component of juxtaglomerular signaling depends on Ca^{2+} signaling in cells other than MD.

An important characteristic of the TGF and renin release mechanism is that furosemide or other loop diuretics effectively block TGF responses (118) and tubular control of renin release (65), although the site of its action has recently become controversial (36). There is even some experimental evidence that furosemide may exert an effect that is independent of its blockade of the MD luminal $Na^+:K^+:2Cl^-$ cotransporter. Therefore, certain effects of furosemide to inhibit renin release may be mediated by an interaction of furosemide with cells in the JGA other than MD cells.

Objectives

The regulation of renal microvascular hemodynamics and the release of renin are orchestrated by the spatial and temporal action of a multitude of different cell types in the juxtaglomerular apparatus. The advent of multiphoton fluorescence microscopy and real-time volume rendering has recently allowed us to study this structure in four dimensions at high optical resolution. Given the caveats associated with two-dimensional imaging of structures demonstrating complex positional changes, including alterations in cell volume, tubular and vascular diameters, we found this approach to be a vast improvement over other optical techniques.

Based on conflicting reports in the past regarding the effect of changes in luminal NaCl concentration on macula densa cell volume, we hypothesize that the relative balance of changes in luminal NaCl versus osmolality are critical determinants of macula densa cell volume changes. In contrast to the artificial experimental conditions used in the past, physiological challenges of increased salt delivery to the macula densa lead to cell shrinkage. The water-permeable macula densa window may sense these changes in luminal environment producing sustained alterations cell volume and that may play a role in juxtaglomerular signaling.

We also hypothesize that the initial part of the distal tubule (distal to macula densa plaque) and the adjoining afferent arteriole segment may build a functional signaling unit. This may involve modified distal tubular cells (termed perimacular cells that appear to be unique from thick ascending limb cells). Luminal NaCl concentration (and flow)-dependent intracellular signaling (involving changes in intracellular Ca^{2+} concentration and basolateral membrane potential) in the early distal tubule may result in signaling from the tubule to the afferent arteriole and account for at least a part of tubuloglomerular feedback signaling.

The objectives of the dissertation are:

1. **To establish a novel imaging model to study the juxtaglomerular apparatus in four dimensions at high temporal and spatial resolution.**
2. **To assess the luminal NaCl and osmolality-dependent changes in macula densa and perimacular cell volume.**

3. **To characterize the oscillations in intracellular Ca^{2+} concentration and membrane potential in perimacular cells. We will evaluate the effects of luminal NaCl concentration and luminal osmolality on the pattern of oscillations in intracellular Ca^{2+} concentration and membrane potential in these cells.**
4. **To determine the role of intracellular Ca^{2+} and membrane potential signaling in perimacular cells in the luminal sodium chloride concentration-dependent regulation of afferent arteriole activation.**

Methods

Materials All materials were purchased from Sigma (St Louis, MO) unless otherwise stated. Fluo-4/AM, fluo-3/AM and bis-(1,3-dibutylbarbituric acid) trimethine oxonol [$DiBAC_4(3)$] were obtained from Molecular Probes Inc. (Eugene, OR); fura-2 was from Teflabs (Austin, TX).

Isolated perfused preparation

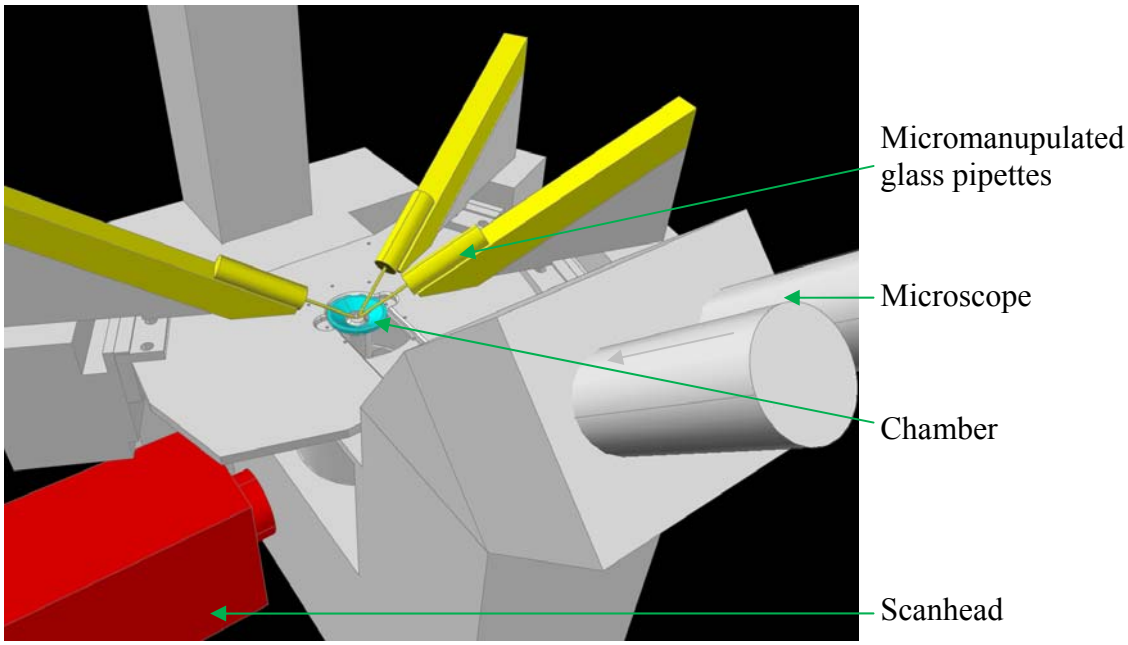

Figure 5 Schematic image showing the setup used to image the isolated living glomeruli. A thermoregulated chamber is mounted onto the stage of an inverted microscope and a custom built micromanipulated set of glass pipettes are used to immobilize the glomerular preparations and cannulate the tubular and arteriolar elements.

Isolated perfused cortical thick ascending limb-distal tubule with attached glomerulus and simultaneously perfused afferent arteriole The animal protocol used in these studies was approved by the Institutional Animal Care & Use Committee at the University of Alabama at Birmingham or at the Medical University of South Carolina, Charleston, SC. Superficial afferent arterioles with glomeruli and associated tubular

segments containing the cTAL and DT were microdissected from rabbit kidneys and perfused *in vitro* using methods similar to those described previously (50). Specifically, the animals were anesthetized with intramuscular ketamine/xylozine, euthanized by intracardiac barbiturate injection or decapitation. After harvesting, the left kidney was sliced into coronal sections and then subjected to hand dissection. Dissection was performed at 4°C in a low-NaCl-containing dissection solution (Table 1) in a custom designed Peltier-cooled dissection station equipped with a stereomicroscope. After transfer to a chamber that was mounted on the microscope, the arteriole and tubule was cannulated; the arteriole and tubule were perfused with bath and perfusion solutions, respectively. The preparations were bathed in the bath solution continuously aerated with 100% O_2 and exchanged at a rate of 1 ml/min. All experiments were conducted at 37°C.

Experimental procedures

Luminal perfusion and the exchange of solutions was achieved by a constant gravity-driven flow within a pressurized system (50). The estimated baseline tubular flow was 20 nL/min. To assess the effect of changes in $[NaCl]_L$ on the epithelial calcium signaling, the perfusate was changed from low salt to high salt solution with concomitant alterations in osmolality (Table 1) and then back to control. This procedure was performed at the beginning and at the end of each experiment, and the results of any test procedures performed between these periods were normalized to the average of these controls.

Table 1 Composition of experimental solutions. Values are given in mmol/L. The pH of all solutions will be set to 7.4 at 37°C.

	Dissection	**Perfusion Low NaCl**	**Perfusion High NaCl**	**Bath**
NaCl	25	−	80	125
KCl	5	−	−	5
Na_2HPO_4	1.6	1.6	1.6	1.6
NaH_2PO_4	0.4	0.4	0.4	0.4
$CaCl_2$	1.5	−	−	1.5
$MgSO_4$	1	1	1	1
Glucose	5	5	5	5
K gluconate	−	5	5	−
Ca gluconate	−	1.5	1.5	−
NMDG-cyclamate	125	±	±	−
$NaHCO_3$	−	−	−	22
HEPES	10	25	25	−
CO_2 (%)	−	5	5	5

Multiphoton fluorescence microscopy

Multiphoton microscopy is a technique in fluorescence microscopy, in which nonlinear fluorescence excitation is strictly confined to the optical section by the process of multiphoton absorption. During the ~100 femtosecond laser pulse, photon density becomes sufficiently high, so that two photons are absorbed simultaneously by the fluorophore. For example, fluo-4, which has an excitation wavelength at 494 nm, is excited at 800 nm using multiphoton microscopy. Importantly, minimal excitation of the fluorophore above or below the focal plane takes place and hence minimal bleaching of the fluorophore will occur in the bulk of the sample. Longer time periods of continuous tissue scanning is possible which provides for an environment well suited for real-time imaging. Longer wavelengths allow for deeper penetration into tissues, while avoiding the deleterious effects of conventional ultraviolet illumination on living specimens.

The preparations were loaded with the acetoxymethyl ester conjugates of the intracellular calcium-sensing dyes fluo-4 or fluo-3 (10^{-5} mol/L) or cell membrane-staining dye TMA-DPH added to the arterial and tubular perfusates and to the bath. The dyes were excited at 800 nm using a Verdi 5-watt diode-pumped, frequency-doubled Nd:vanadate pump laser and a Mira 900 mode-locked titanium-sapphire femto second pulsed laser (Coherent, Santa Clara, CA), coupled to an inverted microscope and Leica confocal imaging system (Leica Microsystems, Heidelberg, Germany). The bandwidth at half-maximum intensity was ~ 7.4 nm. We utilized a 6.25 to 12.5 % neutral density filter at the entry into the microscope. Day-to-day calibration of the acquisition system was performed by scanning calibration beads (Molecular Probes, Eugene, OR) in xyz mode with preset detection settings and determining the sum of intensity values recorded from the beads. Fluorescence emission was detected in xyzt mode using a Leica 100x objective at 515 or 430 nm. In other experiments the preparation was loaded with the membrane potential-sensitive dye $DiBAC_4(3)$, added to the bath (10^{-5} mol/L), and imaged at emission wavelengths of 500 and 600 nm. $DiBAC_4(3)$ fluorescence ratio was used as an index of membrane polarization state, with increases indicating membrane depolarization (13).

Table 2 Properties of fluorescent dyes to be used in the proposed studies

Dye Name	Emission λ (nm)	Purpose	Special considerations
$DiBAC_4(3)$	500/600	membrane potential	emission ratio imaging
Fluo-4	515	cytosolic calcium	
Fura-2	510	bulk cytosolic calcium	excitation ratio imaging
TMA-DPH	430	cell membrane	

Wide-field fluorescence microscopy

cTAL-DT tubular segments were loaded with intracellular calcium-sensing dye fura-2 by adding fura-2/AM (10^{-5} mol/L) or volume-sensing dye calcein/AM (10^{-5} mol/L), dissolved in dimethyl sulfoxide containing 15 % w/v pluronic acid, to the

luminal perfusate. Loading required ~ 15 min. $[Ca^{2+}]_i$ was measured in fura-2-loaded epithelial cells with dual-excitation wavelength fluorescence microscopy (PTI, Lawrenceville, NJ) using a Nikon S Fluor 40x objective and a cooled SenSys charge-coupled camera (Photometrics, Tucson, AZ). Fluorescence was measured at an emission wavelength of 510 nm in response to excitation wavelengths of 340 and 380 nm alternated by a computer-controlled chopper assembly. The autofluorescence-corrected 340 nm-to-380 nm ratios were converted to $[Ca^{2+}]_i$ values using the equation of Grynkiewicz *et al.* (31). For cell volume measurements, fluorescence was measured at an emission wavelength of 530 nm in response to an excitation wavelength of 495 nm. The spontaneous decline in fluorescence intensity was corrected for by linear curve-fitting and normalization.

Image analysis

Volume-rendering was performed with a custom-compiled version of Voxx (Indiana Center for Biological Microscopy, Indianapolis, IN) (18) or Imaris (Bitplane, Zurich, Switzerland) software. Intensity-based segmentation was done using Amira (Mercury Computer Systems, Chelmsford, MA). Matlab (Mathworks, Natick, MA) was utilized for frequency domain analysis (112). The image showing the cumulative increases in fluorescence ratio during the course of an experiment (Figure 14) was generated from a time-lapse image stack by subtracting each image form from the following one, taking the absolute value of each difference image, and then generating a summed image of the stack. Pseudo-linescan images and annotated movies were generated with ImageJ (National Institutes of Health, Bethesda, MD) and Flash (Macromedia, San Francisco, CA) software, respectively.

Statistical analyses

Data are expressed as individual values and means ± SE. Statistical analysis was performed with paired t-test or ANOVA and Dunnett's or Bonferroni's test.

RESULTS

Assessment of epithelial cell volume changes

Effect of increases in $[NaCl]_L$ on MD cell volume as assessed by cytosolic dye concentration

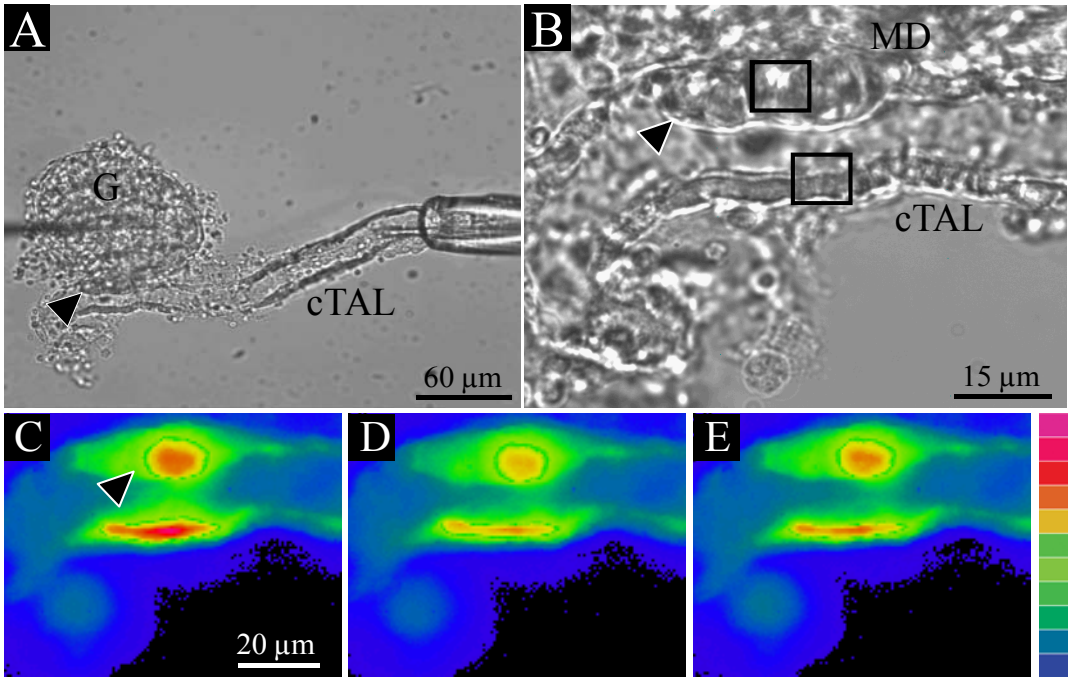

Figure 6 *(A)* and *(B)* Low-power and high-power bright-field images of the isolated perfused cortical thick ascending limb (cTAL)-glomerulus (G). The squares represent regions of interest windows in macula densa (MD) and cTAL cells. *(C)* to *(E)* Wide-field fluorescence images demonstrating the effect of alterations in $[NaCl]_L$ (shown in mmol/l below the images) at constant osm_L (indicated in mOsm/kg H_2O) on calcein fluorescence intensity. The color scale spans from 0 to 2816 intensity units. Arrowhead denotes macula densa plaque.

One approach to determine changes in cell volume is to use the fluorescent probe calcein which can be loaded into cells as an ester form and is trapped inside the cells upon cleavage of the methyl ester.

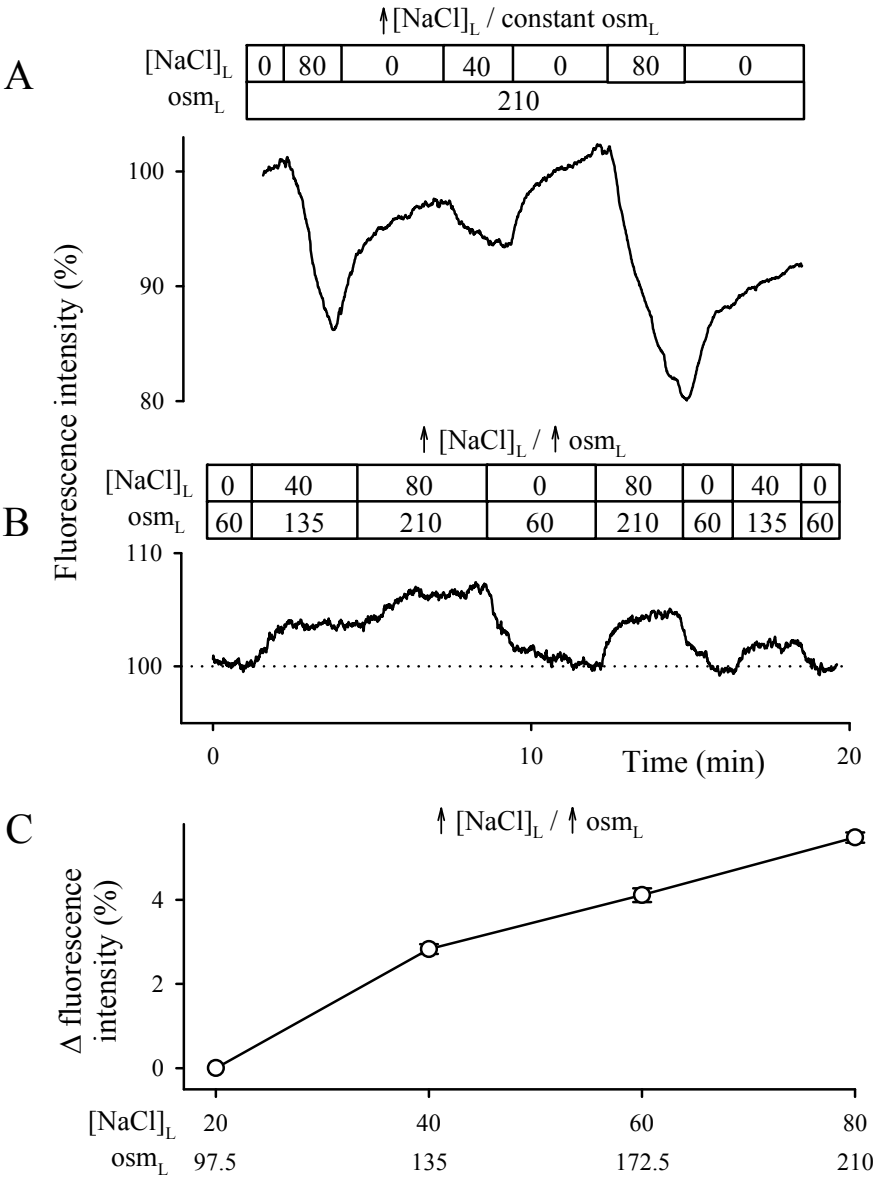

Figure 7 Representative tracings of calcein fluorescence intensity recorded from macula densa plaques upon changes in $[NaCl]_L$ (shown in mmol/l above the tracings) *(A)* at constant osm_L (in mOsm/kg H_2O) and *(B)* with concomitant changes in osm_L. *(C)* Dose-response relationship between $[NaCl]_L$ and calcein fluorescence intensity in macula densa cells upon concomitant alterations in osm_L (n = 4 - 9; all values are different from each other, $p < 0.05$).

Unlike fura-2 or other ionic probes, this dye is not sensitive to changes in intracellular ionic composition. However, when cells swell or shrink, changes in calcein dye concentration can be used as an index of alterations in cell volume. For example, an increase in cell volume is expected to result in a dilution of the dye and a decline in fluorescence. Studies were performed to compare cell volume responses in macula densa versus adjacent cTAL cells (Figure 6). Increases in osm_L caused increases in calcein fluorescence, while decreases in osm_L led to decreases in intensity, indicating an inverse relationship between cell volume and calcein fluorescence intensity. As shown in Figure 7A, increases in $[NaCl]_L$ from 0 to 80 mmol/l at constant osm_L of 210 mOsm/kg H_2O produced reversible, dose-dependent decreases in calcein intensity in the macula densa cells, suggesting reversible cell swelling. Luminal application of 10^{-4} mol/L furosemide, inhibitor of Na^+:$2Cl^-$:K^+ cotransporter, reduced the magnitude of changes in calcein intensity upon increases in $[NaCl]_L$ at constant osm_L by 83 ± 11 % (n = 6; $p < 0.05$). In contrast, parallel increases in $[NaCl]_L$ and osm_L from 0 to 80 mmol/l and from 60 to 210 mOsm/kg H_2O (Figure 7B) caused increases in calcein fluorescence, indicating cell shrinkage. As shown in Figure 7C, concomitant increases in $[NaCl]_L$ and osm_L produced dose-dependent decreases in macula densa cell volume. The comparison of volume responses to changes in luminal fluid composition between macula densa and cTAL produced strikingly different responses. As shown in Figure 8A, both cell types produced cell swelling in response to increases in $[NaCl]_L$ at constant osm_L. In contrast, increases in both $[NaCl]_L$ and osm_L produced cell shrinkage in macula densa cells and cell volume increase in cTAL cells. Interestingly, cell volume responses in macula densa cells were sustained, while the volume responses in cTAL were transient, suggesting active volume-regulatory mechanisms in cTAL cells (Figure 7B).

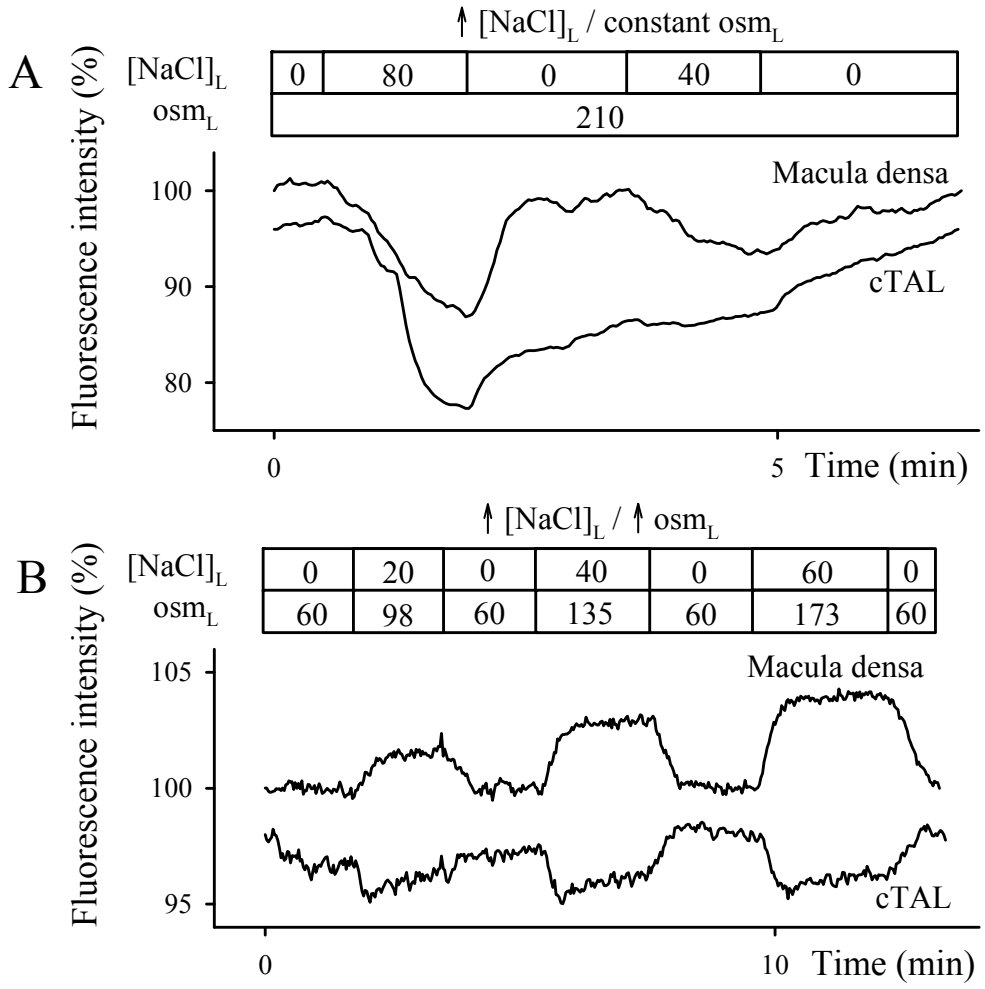

Figure 8 Representative tracings of calcein fluorescence intensity recorded from macula densa plaques and cortical thick ascending limb cells (cTAL) upon changes in $[NaCl]_L$ (shown in mmol/l above the tracings) *(A)* at constant osm_L (in mOsm/kg H_2O) and *(B)* with concomitant changes in osm_L. Cell volume changes in macula densa cells were sustained, cTAL cells exhibited cell volume regulatory responses.

Effect of increases in $[NaCl]_L$ and osm_L on MD cell volume as assessed by cell membrane imaging

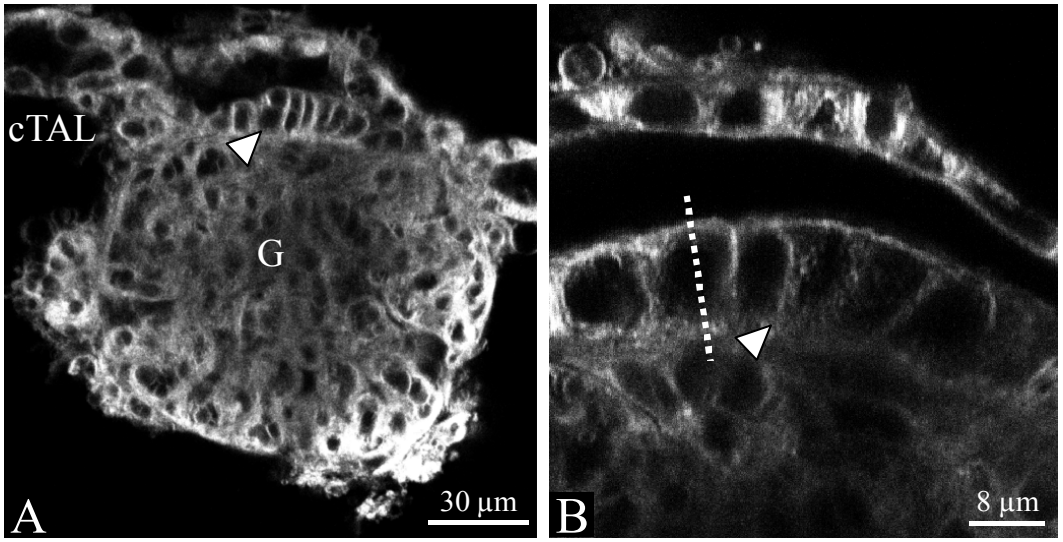

$[NaCl]_L$	0	80	0	0	80	0	0	0	0
osm_L	210	210	210	60	210	60	60	210	60

Figure 9 Representative *(A)* low-power and *(B)* high-power multiphoton confocal fluorescence images of the isolated perfused cortical thick ascending limb (cTAL)-glomerulus (G) visualized with membrane-dye TMA-DPH. White arrowhead denotes macula densa plaque. *(C)* to *(E)* Psedolinescan images generated from time-series images along the dotted line marked on panel *(B)* demonstrating the effects of alterations in $[NaCl]_L$ (in mmol/l; underneath the images) and/or osm_L (in mOsm/kg H_2O) on macula densa cell height. Black arrowhead and arrow denote apical and basolateral membrane of the macula densa cell, respectively.

As determined by visualizing cell membranes with a membrane-staining dye TMA-DPH (Figure 9) and multiphoton excitation confocal microscopy, increases in $[NaCl]_L$ from 0 to 80 mmol/l at constant osm_L of 210 mOsm/kg H_2O produced

reversible swelling of macula densa cells with an increase in cross sectional area of 24 ± 4 %, while parallel increases in $[NaCl]_L$ and osm_L from 0 to 80 mmol/l and from 60 to 210 mOsm/kg H_2O, respectively, caused reversible shrinkage of macula densa cells (Figure 9C, Figure 9D, Figure 10 and Figure 11) with a decrease in cross sectional area of 10 ± 2 % (Figure 10). These changes in macula densa cross sectional area were caused by increases in macula densa cell height.

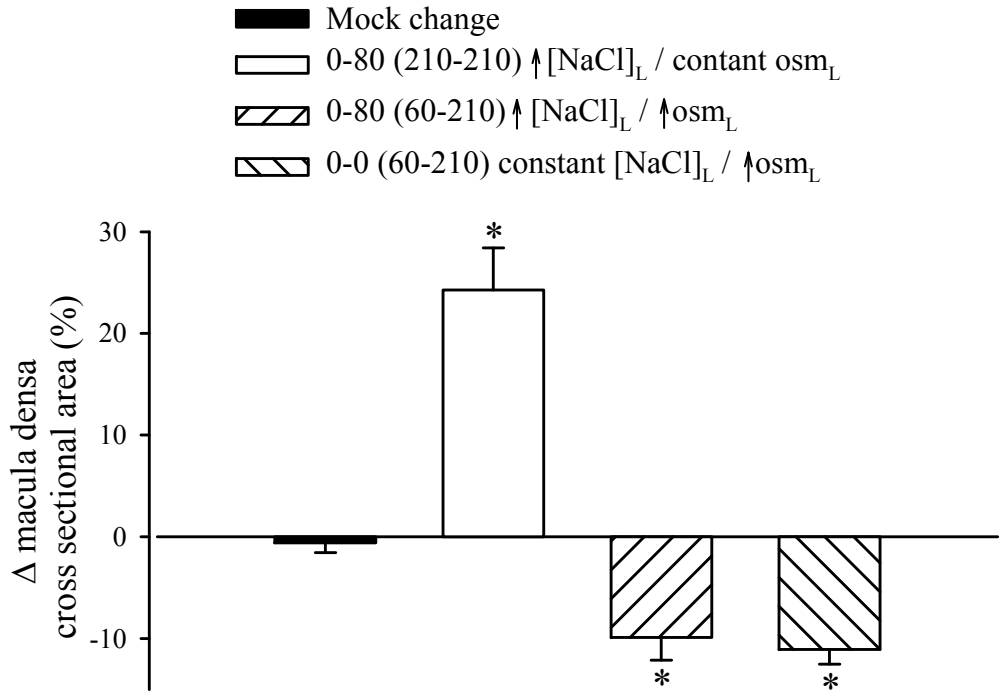

Figure 10 Effect of modulation of $[NaCl]_L$ (in mmol/l; see legend) and/or osm_L (in mOsm/kg H_2O; see legend in parenthesis) on the macula densa cross sectional area (n = 6; * $p < 0.05$ as compared to values obtained with mock changes).

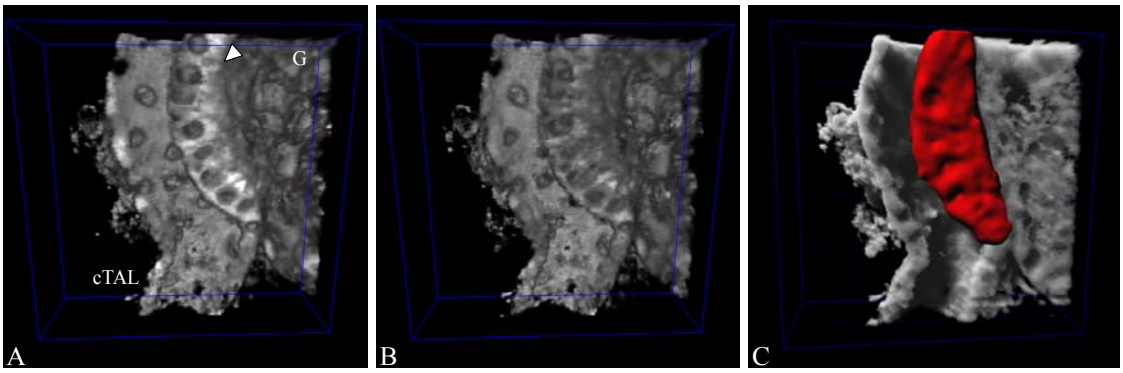

Figure 11 Four-dimensional volume-rendering and segmentation of the isolated perfused cTAL-glomerulus (G). *(A)* to *(B)* Representative volume-rendered images of the preparation visualized with cytosol-labeling dye $DiBAC_4(3)$ demonstrating the effect of concomitant reductions in $[NaCl]_L$ and osm_L from *(A)* 80 to *(B)* 0 mmol/l and from 210 to 60 mOsm/kg H_2O, respectively. White arrowhead denotes macula densa plaque. Note the swelling of macula densa cells. *(C)* Representative volume-rendered image of the same preparation merged with the intensity-segmented surface object of the macula densa plaque (red). As measured with isosurface tracking, macula densa cell volume increased from 28152 to 29510 μm^3 upon a decrease in $[NaCl]_L$ and osm_L from 80 to 0 mmol/l and from 210 to 60 mOsm/kg H_2O. Gridlines are 20 µm apart.

Effect of $[urea]_L$ on MD cell volume

Under normal physiological conditions, changes in osm_L occur predominantly through either alterations in $[NaCl]_L$ or $[urea]_L$. Studies in Figure 12 compare the changes in macula densa cell volume with addition of either NaCl or urea. As shown in Figure 12B, increases in $[urea]_L$ produced cell shrinkage, although at comparable osmotic concentration it was less effective than NaCl. Elevations in $[urea]_L$ from 0 to 160 mmol/l (60 to 217 mOsm/kg H_2O) caused a reversible, dose-dependent increase in calcein fluorescence of 2.7 ± 0.6 %.

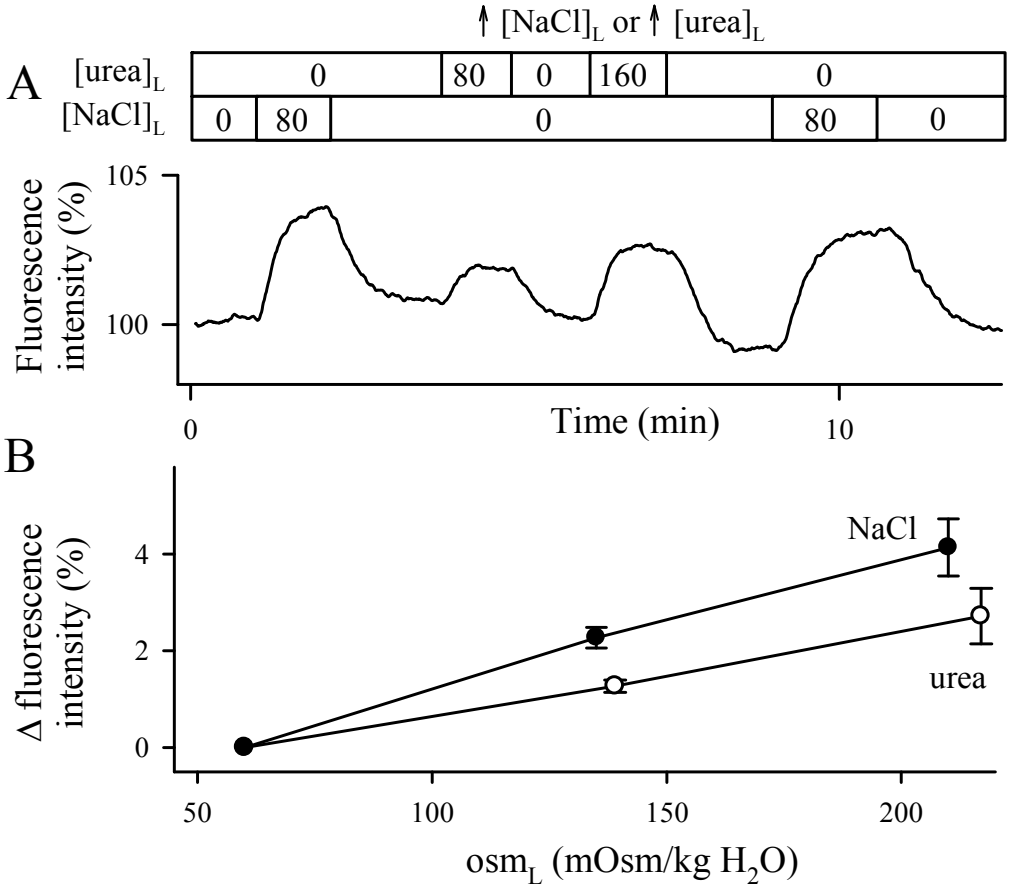

Figure 12 *(A)* Representative tracing of calcein fluorescence intensity recorded from macula densa cells demonstrating the effects of modulation of $[urea]_L$ or $[NaCl]_L$ (shown in mmol/l above the tracing) on calcein fluorescence with concomitant alterations in osm_L. *(B)* Effect of concomitant increases in $[urea]_L$ or $[NaCl]_L$ and osm_L (indicated in mOsm/kg H_2O) on macula densa calcein fluorescence intensity (n = 5).

Assessment of epithelial intracellular calcium concentration

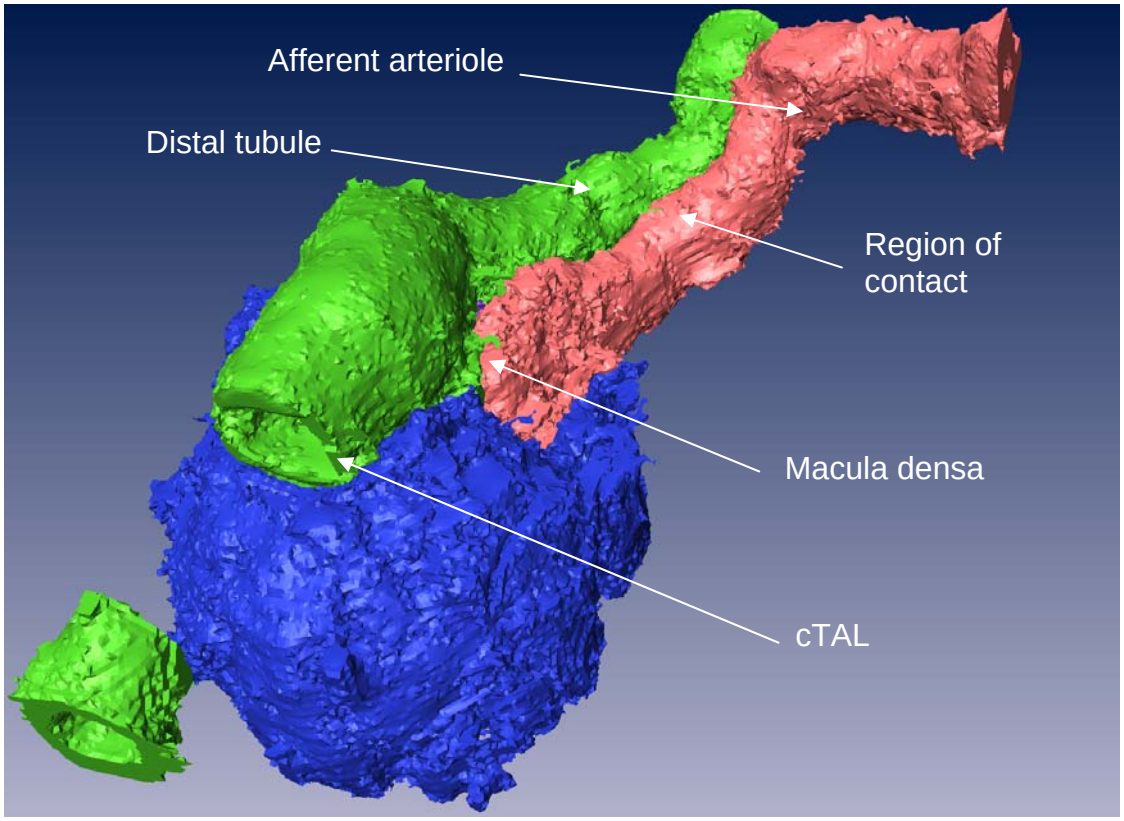

Figure 13 Image demonstrating extensive region of contact between distal tubule and afferent arteriole. Double-perfused JGA preparation was loaded with fluo-3 and imaged with multiphoton microscopy. 3-dimensional reconstruction and segmentation was performed with Amira. Portion of the cTAL has been removed to gain insight into the tubule.

In early electronic microscopic studies by Barajas *et al.* (1) an extensive region of contact was shown to exist between the terminal segment of cTAL and the efferent arteriole. However, the possible juxtaposition of the initial portion of the distal tubule (DT) with the afferent arteriole has not been shown in rabbits. To further study the possible functional association of the DT and afferent arteriole, we isolated cTAL-DT-glomerular preparations with the afferent arteriole from rabbit kidney taking care to maintain the arteriole-tubular relationship intact. As shown in the representative intensity-segmented and pseudo-colored 3-dimensional reconstruction in Figure 13,

there is a ~ 100 μm-long area of contact between the early DT and the terminal portion of the afferent arteriole.

Certain JGA elements demonstrate oscillations in $[Ca^{2+}]_i$ and V_{bl}.

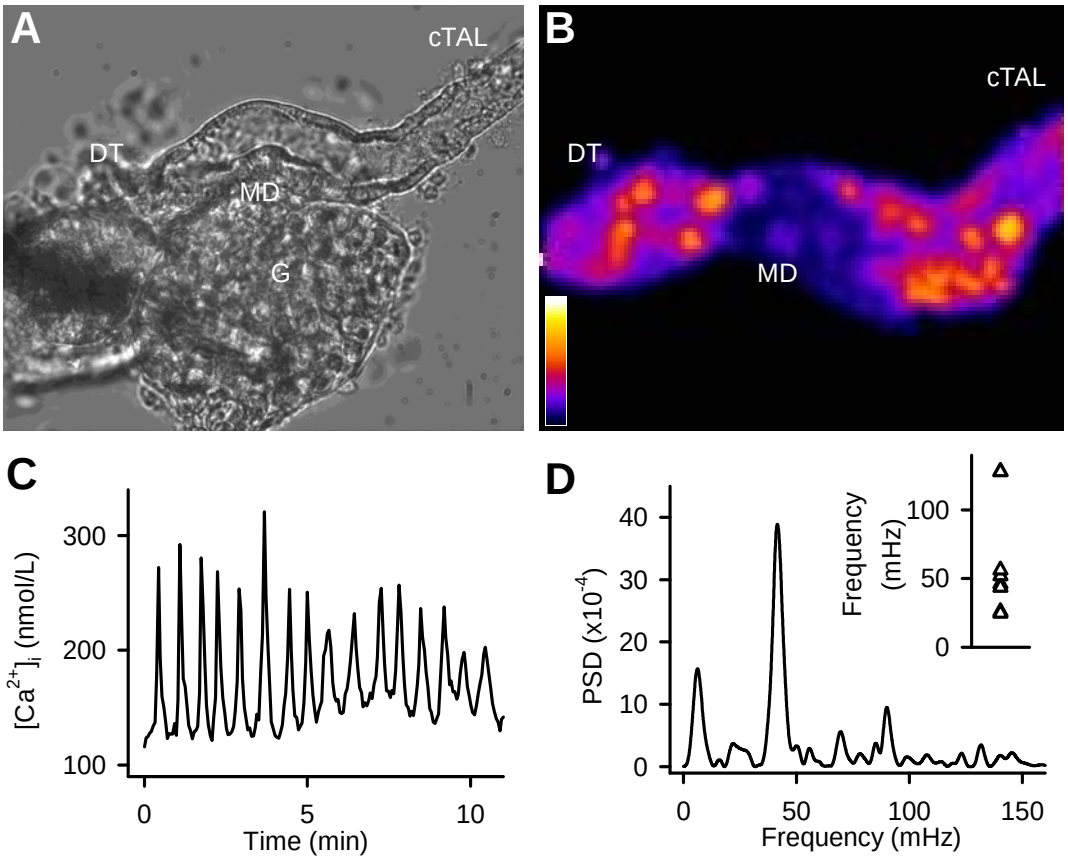

Figure 14 Wide-field fura-2 imaging of the isolated perfused cortical thick ascending limb-distal tubule preparation with attached glomerulus. *(A):* Bright-field photomicrograph demonstrating the cortical thick ascending limb (cTAL), the distal tubule (DT), the macula densa plaque (MD) and the glomerulus (G). The tubule was cannulated and perfused from the cTAL end. *(B):* Image showing the cumulative increases in intracellular calcium concentration ($[Ca^{2+}]_i$) during the course of the experiment. Note that the tubular epithelial cells in the terminal segment of the cTAL and in the early portion of the DT demonstrate spontaneous oscillations in $[Ca^{2+}]_i$, while the macula densa cells and the proximal cTAL segment do not. *(C):* Representative $[Ca^{2+}]_i$ recording from a cell in the terminal cortical thick ascending limb. *(D):* Representative power spectrum density (PSD) plot of the $[Ca^{2+}]_i$ recordings in the frequency domain. The Nyquist frequency was 164 mHz. Inset demonstrates the position of power spectrum peaks (with a relative power of at least 40 %) on the frequency domain.

In the course of measuring $[Ca^{2+}]_i$ in macula densa cells, we observed the presence of epithelial cells that appear to exhibit large spontaneous oscillations in $[Ca^{2+}]_i$. To characterize this activity, we utilized ratiometric fluorescence imaging with fura-2 under baseline conditions of low luminal sodium chloride concentration ($[NaCl]_L$) of 20 mmol/L. Interestingly, in 78 % of the 55 preparations studied, a group of cells in the initial DT and/or terminal cTAL demonstrated spontaneous oscillations in $[Ca^{2+}]_i$. Occasionally, oscillations were also observed in more proximal segments of the cTAL or more distally in the DT.

To further characterize the intracellular Ca^{2+} signaling in the epithelial cells of the early DT, 4-dimensional imaging was performed. As shown on Figure 15 and, the cells of the tubular epithelium in the proximity of the macula densa plaque in the DT, cTAL and also in the region opposite to the macula densa plaque demonstrated spontaneous oscillations in $[Ca^{2+}]_i$. However, macula densa cells did not exhibit detectable oscillations (Figure 14B). In 28 of the 39 preparations, oscillations were highly regular and monomorph, similar to that shown on Figure 14C. Analysis of the Ca^{2+} recordings in the frequency-domain (Figure 14D) revealed a dominant oscillatory

frequency of 63 ± 15 mHz (n = 8). Oscillations in $[Ca^{2+}]_i$ in the perimacular cells were abolished by omission of Ca^{2+} from the bath solution (data not shown).

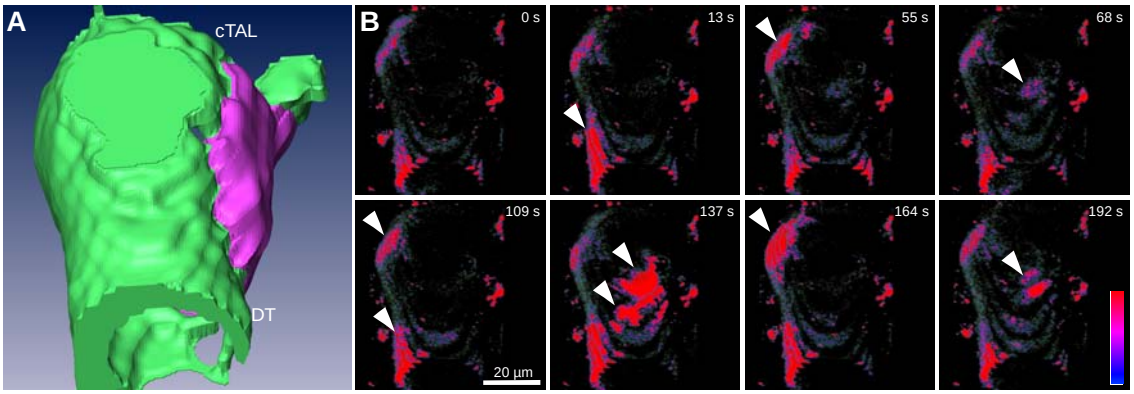

Figure 15 Four-dimensional multiphoton fluorescence imaging of isolated perfused tubular preparation *(A):* Schematic segmentation image showing the topography of the preparation in panel *(B)*. MD is indicated in purple. *(B):* Snapshots from 4-dimensional reconstruction (see movie 1) showing spontaneous intracellular Ca^{2+} spikes (arrowheads) in the tubular epithelial cells in the perimeter of MD at the indicated time points.

We then used the voltage-sensitive dye $DiBAC_4(3)$ to determine whether the oscillatory intracellular calcium signaling is associated with changes in membrane potential. The partition of this particular dye in the plasma membrane is dependent on the transmembrane potential, and by adding to the bath solution only, can be used to detect changes in basolateral membrane potential (V_{bl}) using emission ratiometric fluorescence imaging. As shown on Figure 16C, membrane depolarization with basolateral application of 100 mmol/L potassium chloride led to rapid, reversible increases in fluorescence ratio values. Using this electrical potential sensing dye, we have detected cyclic changes in V_{bl} in the perimacular cells (Figure 16D). To determine if $[Ca^{2+}]_i$ signaling in perimacular cells is dependent on changes in V_{bl}, we administered 100 mmol/L KCl in the luminal perfusate or in the bath to depolarize epithelial cells. As shown in Figure 17, depolarizing the basolateral membrane with potassium chloride reduced $[Ca^{2+}]_i$ in perimacular cells and abolished oscillations in 5 of the 8 preparations.

Interestingly, in half of the experiments the withdrawal of potassium chloride was followed by a large calcium spike, as shown on Figure 17A.

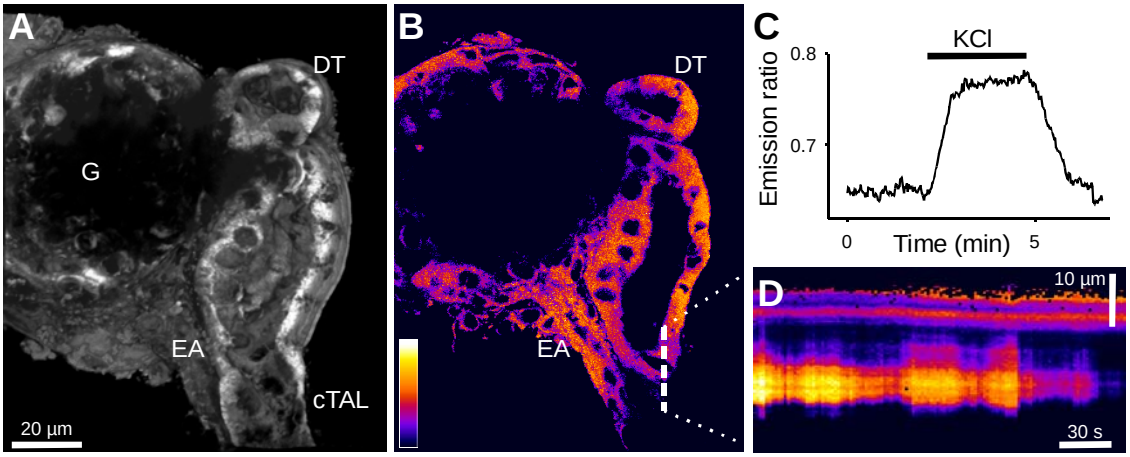

Figure 16 Confocal imaging of membrane potential changes in the isolated perfused cTAL-DT preparation. *(A):* 3-dimensional reconstructed and *(B):* confocal emission ratio images of the preparation loaded with the membrane potential-sensitive $DiBAC_4(3)$ dye. Note the efferent arteriole (EA) and glomerulus (G). *(C):* Graph demonstrating the effect of membrane depolarization by application of KCl (100 mmol/L) in the bath on the emission ratio values obtained from a preparation. *(D):* Pseudo-linescan image along the dashed line on panel *(B)* demonstrating spontaneous oscillations in the membrane potential of a tubular cell in the cTAL.

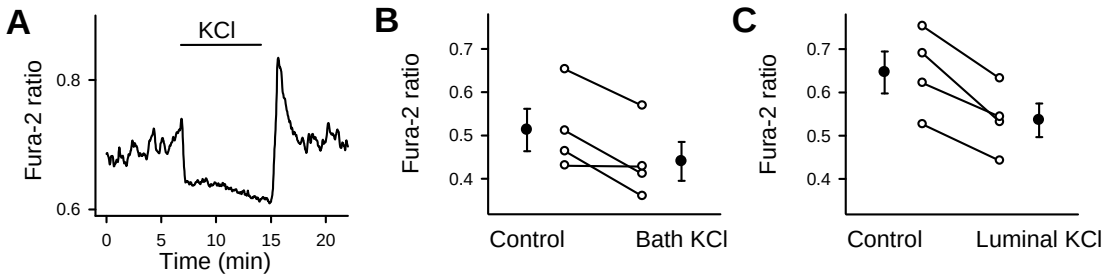

Figure 17 Effect of membrane depolarization on the $[Ca^{2+}]_i$ in the perimacular oscillatory cells. *(A):* Representative fura-2 ratio recording demonstrating the effect of KCl (100 mmol/L from the lumen) on $[Ca^{2+}]_i$ in a perimacular cell located in the terminal portion of the cTAL. *(B)* and *(C):* Effect of *(B)* bath and *(C)* luminal KCl on $[Ca^{2+}]_i$ in perimacular tubular epithelial cells. Open circles denote fura-2 ratio values from individual cells, filled circles show the average values (n = 4, one cell each from every preparation; the values in the control and KCl groups were different from each other; $P < 0.05$).

$[Ca^{2+}]_i$ signaling in perimacular cells is affected by the calcium-sensing receptor

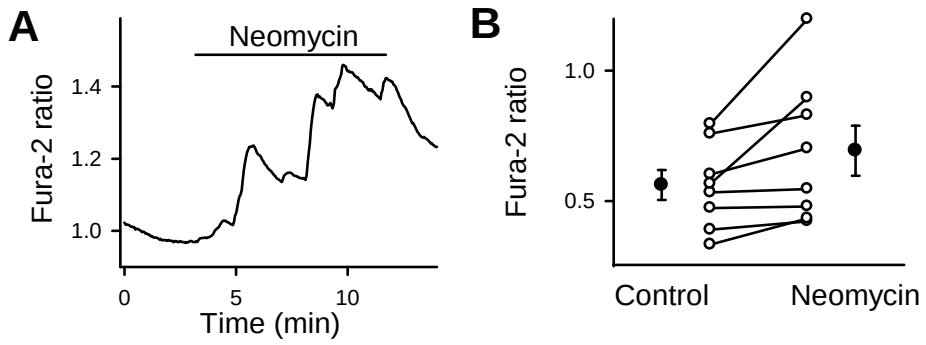

Figure 18 Effect of activation of calcium sensing receptor on $[Ca^{2+}]_i$ in the perimacular oscillatory cells. *(A):* Representative fura-2 ratio recording demonstrating the effect of neomycin, an activator of calcium-sensing receptor ($5x10^{-4}$ mol/L from the bath), on $[Ca^{2+}]_i$ in a perimacular cell located in the terminal portion of the cTAL. *(B):* Effect of neomycin on $[Ca^{2+}]_i$ in perimacular tubular epithelial cells. Open circles denote fura-2 ratio values from individual cells, filled circles show the average values (n = 8, one cell each from every preparation; the values in the control and neomycin groups were different from each other; $P < 0.05$).

Previous immunohistological studies concluded that the calcium-sensing receptor is preferentially expressed in the basolateral membrane of the macula densa plaque and in the epithelial cells around it (89). We hypothesized that the calcium-

sensing receptor might play a role in the generation of calcium oscillations in perimacular epithelial cells. As shown on Figure 18, basolateral application of $5x10^{-4}$ mol/L neomycin, an activator of calcium-sensing receptor produced robust increases in $[Ca^{2+}]_i$ in perimacular cells. Also, we observed a marked increase in perimacular cell oscillation amplitude in 10 of the 14 experiments.

Flow and $[NaCl]_L$-dependent $[Ca^{2+}]_i$ signaling in the perimacular cells

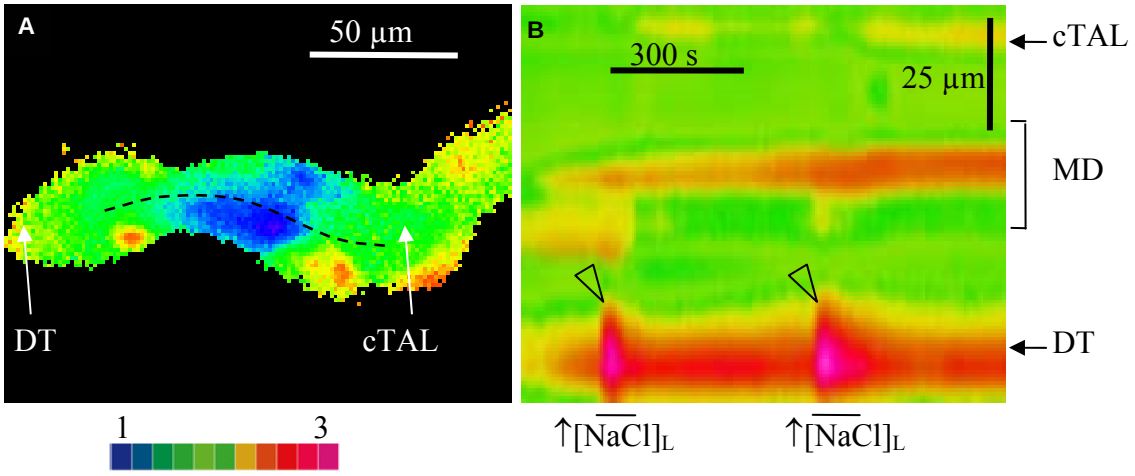

Figure 19 Characteristics of $[NaCl]_L$-dependent changes in $[Ca^{2+}]_i$ in macula densa and perimacular cells. *(A):* Wide-field fura-2 ratio and *(B)*: pseudo-linescan image obtained along the line illustrated on panel *(B).* Note the robust increases in $[Ca^{2+}]_i$ in the early distal tubule upon increases in $[NaCl]_L$ from 0 to 80 mmol/L (arrowheads).

Next we characterized the effect of elevations in $[NaCl]_L$ and osm_L on perimacular cell intracellular calcium signaling. As shown in Figure 19A, Figure 19B, Figure 20C and Figure 20D, an increase in $[NaCl]_L$ from 20 to 80 mmol/L and a concomitant increase in luminal osmolality from 98 to 210 mOsm/kg H_2O resulted in robust, reversible increases in $[Ca^{2+}]_i$ especially in those perimacular cells located in the distal tubule, and very modest changes in macula densa. Also, a reversible increase in oscillation frequency/and intracellular calcium salve (see Figure 20C) was observed upon application of elevated $[NaCl]_L$.

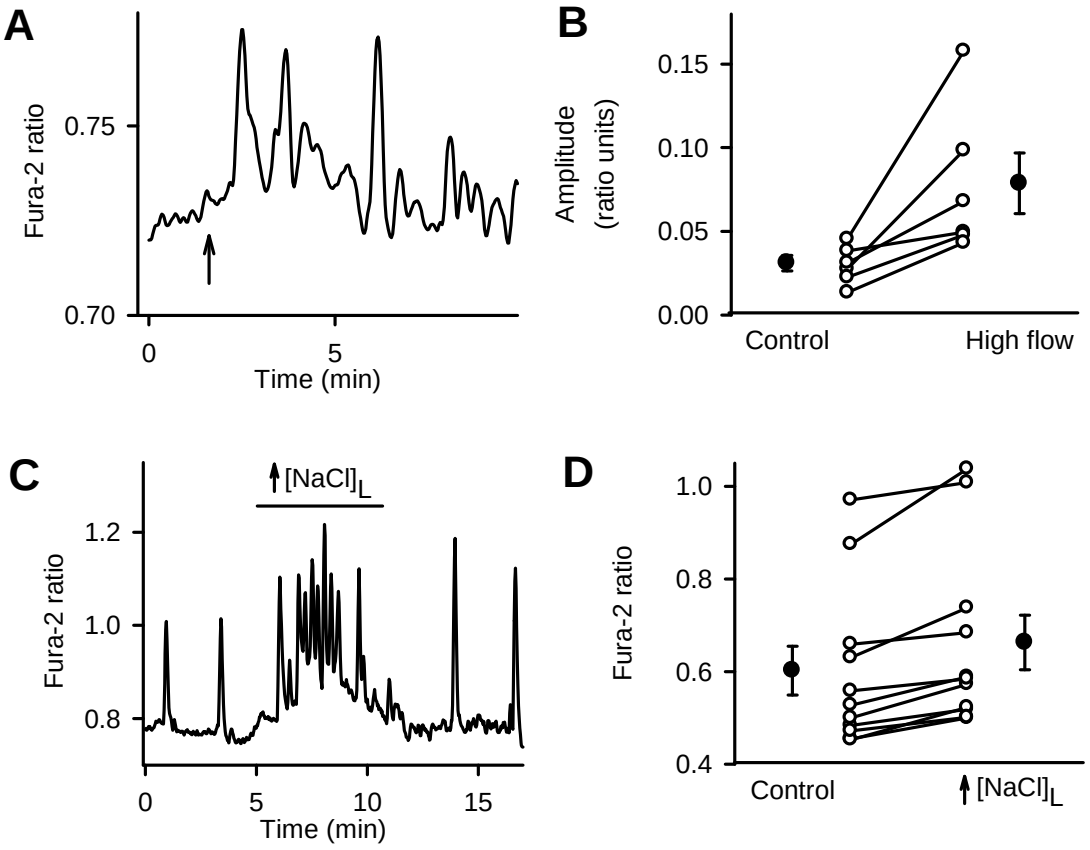
A
Fura-2 ratio
0.75
0.70
0
5
Time (min)
B
Amplitude
(ratio units)
0.15
0.10
0.05
0.00
Control
High flow
C
[NaCl]L
Fura-2 ratio
1.2
1.0
0.8
0
5
10
15
Time (min)
D
Fura-2 ratio
1.0
0.8
0.6
0.4
Control
[NaCl]L

Figure 20 Effect of tubular flow and luminal sodium chloride concentration $[NaCl]_L$ on $[Ca^{2+}]_i$ in perimacular oscillatory cells. *(A):* Representative fura-2 ratio recording demonstrating the effect of elevated tubular flow from 20 to 40 nL/min (onset at the time point indicated by arrow) on the intracellular calcium dynamics in a perimacular cell located in the terminal portion of the cTAL. *(B):* Effect of elevations in tubular flow on the amplitude of oscillations in $[Ca^{2+}]_i$ in perimacular tubular epithelial cells. Open circles denote fura-2 ratio oscillation amplitude values from individual cells at different tubular flow conditions, filled circles show the average values (n = 6, one cell each from every preparation; the values in the control and high flow groups were different from each other; $P < 0.05$). *(C):* Representative fura-2 ratio recording demonstrating the effect of an increase in $[NaCl]_L$ and osmolality (from 20 to 80 mmol/L and from 98 to 210 mOsm/kg H_2O) on $[Ca^{2+}]_i$ in a perimacular cell located in the early portion of the distal tubule. *(D):* Effect of elevations in $[NaCl]_L$ and osmolality on $[Ca^{2+}]_i$ in perimacular tubular epithelial cells of the early distal tubule. Open circles denote fura-2 ratio values from individual cells, filled circles show the average values (n = 12, one cell each from every preparation; the values in the control and high NaCl groups were different from each other; $P < 0.05$).

Figure 20A and Figure 20B shows the effect of an increase in luminal flow on $[Ca^{2+}]_i$ in perimacular cells. Changing from low to high flow resulted in a significant increase in the amplitude of calcium oscillations in perimacular cells in every preparation. In case of macula densa cells, the increased tubular flow did not produce oscillations, but produced a significant increase in fura-2 ratio in 4 of 8 experiments.

Role of cell volume and $[Ca^{2+}]_i$ in the signaling of NO release and vascular responses

$[Ca^{2+}]_i$ dynamics during juxtaglomerular tubule-to-arteriole paracrine signaling

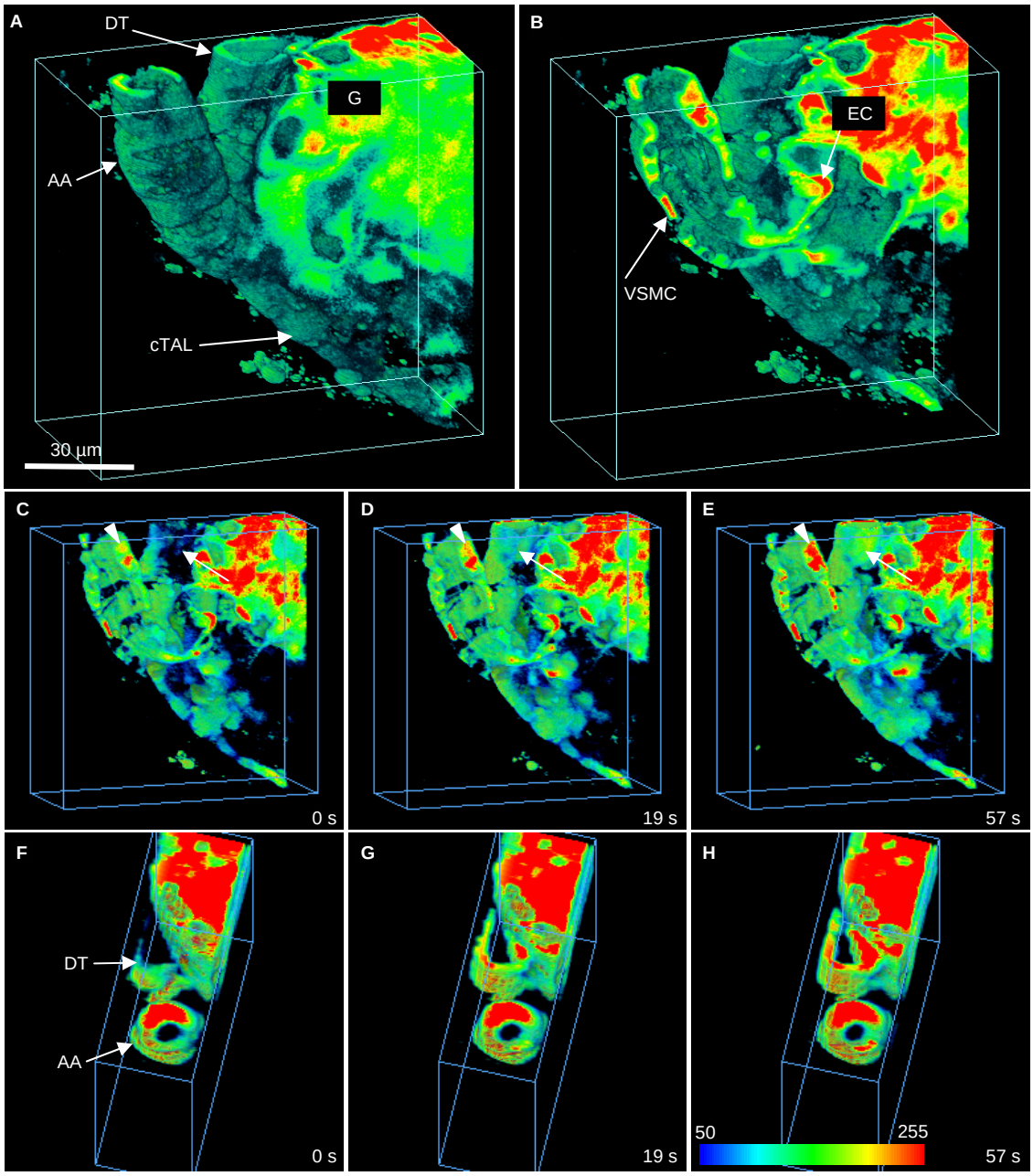
A
DT
G
AA
cTAL
30 µm
B
EC
VSMC
C
0 s
D
19 s
E
57 s
F
DT
AA
0 s
G
19 s
H
50
255
57 s

Figure 21 Four-dimensional imaging of tubule-dependent activation of the afferent arteriole (AA) in situ with multiphoton fluorescence microcopy using Ca^{2+}-sensing dye fluo-4. *(A)* and *(B):* Glomerulus (G) perfused through the AA with attached cortical thick ascending limb (cTAL) and distal tubule (DT). Note the vascular smooth muscle cells (VSMC), endothelial cells (EC). *(C)* to *(E):* Snapshots at time points indicated from 4-dimensional reconstruction demonstrating increased fluorescence in the early ad-glomerular DT (arrows) and concomitant increases in fluorescence in the adjacent VSMCs of the AA (arrowheads) in response to an elevation in tubular luminal NaCl concentration from 0 to 80 mmol/L. *(F)* to *(H):* Snapshots from the axial view of the afferent arteriole showing decreases in vascular luminal diameter (see movie 2 demonstrating reversible changes)**.**

To determine the possible role of intracellular Ca^{2+} signaling in perimacular cells in the $[NaCl]_L$-dependent regulation of afferent arteriole activation, we cannulated and perfused the cTAL-DT segment and the afferent arteriole simultaneously and assessed the activation of the afferent arteriole with Ca^{2+}-sensitive dye fluo-4 and four-dimensional multiphoton excitation microscopy. As shown in the representative snapshots in Figure 21, elevations in $[NaCl]_L$ resulted in marked increases in $[Ca^{2+}]_i$ in the early DT and also in the adjacent afferent arteriole. The increases in $[Ca^{2+}]_i$ in the afferent arteriole were associated with reversible reductions in luminal diameter of the afferent arteriole, best visualized in the axial reconstruction view of the experiment (Figure 21F-H).

Discussion

Cell volume studies

The first part of the presented studies demonstrated that changes in cell volume in macula densa cells critically depend on the chosen experimental conditions. In spite of this finding, three major conclusions can be drawn from this work. First, increases in $[NaCl]_L$ under physiological relevant conditions result in macula densa cell shrinkage. Second, consistent with previous observations (28, 48) and in contrast to the adjacent

cTAL cells, the apical membrane of macula densa cells is permeable to water. Third, macula densa cells lack effective cell volume regulatory mechanisms. As reported previously by others and also by our group, (63, 64, 84) increases in $[NaCl]_L$ at constant or close-to-constant osm_L (~300 mOsm/kg H_2O) produce macula densa cell swelling. This has been reconfirmed in our current studies using both the volume-sensitive dye calcein and also by visualizing cell membranes of macula densa cells with multiphoton fluorescence microscopy. Increases in $[NaCl]_L$ at constant osm_L also produced reversible decreases in calcein intensity in cTAL cells, suggesting cell swelling.

In contrast, increasing $[NaCl]_L$ and osm_L concomitantly caused increases in calcein fluorescence, indicating shrinkage of macula densa cells. In the presence of concomitant changes in $[NaCl]_L$ and osm_L, there was a linear relationship between $[NaCl]_L$ and cell volume between 20 to 80 mmol/l $[NaCl]_L$ (Figure 7). Also, as shown in Figure 9 and Figure 11, concomitant increases in $[NaCl]_L$ and osm_L led to modest decreases in cell height and a shrinkage of macula densa cells. Interestingly, in both calcein and membrane staining experiments, concomitant increases in $[NaCl]_L$ and osm_L produced reversible swelling of cTAL cells. Thus these studies report a fundamental difference in the way macula densa and cTAL cells respond when both $[NaCl]_L$ and osm_L are altered concurrently.

We interpret these data as follows: it is firmly established that both macula densa and cTAL cells possess the apical $Na^+:2Cl^-:K^+$ cotransporter (56). Thus, increases in $[NaCl]_L$ will result in uptake of NaCl into both cell types. Increasing intracellular [NaCl] would then result in a relative increase in the osmotic gradient for water entry into the cell. Presumably, both cTAL and macula densa cells possess a finite basolateral water permeability so that water can enter across the basolateral membranes. Studies by Gonzalez *et al.* (28) have shown that the osmotic water permeability of the macula densa basolateral membrane is about 13 times higher than that of the apical membrane. Thus a steady-state increase in NaCl entry would lead to water uptake and cell swelling, which would be blocked by furosemide, an inhibitor of the $Na^+:2Cl^-:K^+$ cotransporter. Furosemide blocked the cell-volume changes by 83 %, a value that is in accordance with earlier studies indicating that ~ 80 % of apical Na^+ entry into the macula densa cells occurs via the $Na^+:2Cl^-:K^+$ cotransporter, while the $Na^+:H^+$ exchanger is

responsible for the remainder (79). However, the difference between macula densa and cTAL cells appears to be that whereas the apical membrane of cTAL cells is impermeable to water, macula densa cells exhibit finite water permeability. Thus when both $[NaCl]_L$ and osm_L are increased, cTAL cells still swell, because there is no "effective change" in the lumen to cell osmotic gradient in spite of changes in osm_L. While in macula densa cells, the finite apical water permeability allows for an osmotic gradient to form across the apical membrane and, in the presence of elevated apical osmolality, the relative movement of water from cell to lumen. Although the present studies did not measure water permeability of macula densa cells, per se, the conclusion that can be reached is that the apical membrane of these cells is permeable enough to counteract the effects of enhanced NaCl entry. This is in accordance with earlier studies indicating that the water permeability of macula densa cells is ~ 12 times higher than that of the thick ascending limb (12, 28). Thus the overall effect of increases in $[NaCl]_L$ (in the absence of mannitol or other osmotic agents) is to elicit cell shrinkage in macula densa cells. Interestingly, the fractional change in calcein fluorescence intensity (5.5 %, Figure 7) was smaller than the observed change in macula densa cross sectional area (10 %, Figure 10). Although there might exist several explanations for this, one possible reason is that changes in macula densa cell volume do not necessarily parallel changes in macula densa cell height. An example of this is an earlier study (48) demonstrating concurrent heightening of macula densa cells with widening of the intercellular spaces.

These results suggest that there is a finite permeability for water across the apical membrane of macula densa cells. Physiologically, as flow is increased through the cTAL, the augmented flow would produce elevations in osm_L due primarily to increases in $[NaCl]_L$ and $[urea]_L$. Effective changes in the osmotic gradient across cells is related to the osmotic reflection coefficient of a particular solute. Thus in spite of the fact that NaCl is transported into macula densa cells, its osmotic reflection coefficient across the apical membrane of macula densa cells is presumably high as it is in most cell types (88). This means that the osmotic driving force generated by Na^+ and Cl^- is almost equivalent to their concentration. However, despite some exceptions, such as the thin ascending limb of the TAL (12), most cells have a finite permeability to urea and therefore a lower reflection coefficient. This is entirely consistent with the results

obtained in the current studies where an equal osmotic concentration of urea was less effective in causing cell shrinkage than NaCl.

One of the more interesting findings of the present studies is the lack of volume regulation in macula densa cells. Persson and his coworkers observed some signs of volume regulatory changes (28, 63, 64) in macula densa cells upon alterations in osmolality, but also reported, that increases in $[NaCl]_L$ lead to sustained changes in cell volume (28). Thus, there is conflicting information concerning the ability of macula densa cells to regulate cell volume. In response to cell swelling or shrinkage, most cells exhibit volume regulatory response. This is the case for cTAL cells Figure 8B) where elevated $[NaCl]_L$ results in cell swelling (decrease in calcein fluorescence) followed by a time-dependent return toward control levels. In most cells this regulatory volume decrease (RVD) is due to transport of osmotically active solutes from cell to extracellular fluid: chloride and potassium have both been shown to be involved in RVD in other cell types (21).

However, macula densa cells (Figure 8B) show little tendency for volume regulation upon either cell shrinkage or cell swelling. One explanation for this is that previous work (79) indicated that intracellular $[Na^+]$ mirrored changes in $[NaCl]_L$ between 0 and 60 mmol/l. Thus an elevation of $[NaCl]_L$ results in a sustained increase in intracellular $[Na^+]$. If this also applies to other intracellular electrolytes such as chloride and potassium, then it would explain why there is a lack of volume regulation in macula densa cells; i.e. no volume regulatory influx or efflux of osmotically active solutes.

The finding that macula densa cells do not volume regulate is consistent with the role of this unique cell type as the sensor element for the TGF mechanism. In response to changes in the luminal environment there are also sustained responses of basolateral membrane potential, intracellular $[Na^+]$, $[Ca^{2+}]$ and pH. Thus a sustained response to alterations in the luminal environment appears to be a consistent characteristic of macula densa and may be an integral part of TGF signaling. However, a recent study failed to find a difference between the magnitude of *in vitro* afferent arteriole diameter responses to elevations in $[NaCl]_L$ whether the osm_L was maintained constant or was increased concomitantly (62), suggesting that changes in macula densa cell volume might not be directly involved in the TGF signaling process. Since this study was

performed using very low (~ 11 mmol/l) and high (~ 81 mmol/l) $[NaCl]_L$, this finding does not eliminate the possibility that changes in cell volume can influence TGF responses over the physiological range of $[NaCl]_L$ and osm_L. On the other hand, it is now known that macula densa cells are involved in other paracrine or signaling processes. For instance macula densa cells produce both nitric oxide (53, 62) and prostaglandin E_2 (83). Thus it is possible that changes in cell volume may affect the production of these signaling molecules or may alter other, as yet to be identified, function(s) of macula densa. It is also possible that cell volume maybe involved in TGF resetting (100). We speculate that macula densa cell volume changes might play a role in TGF resetting under conditions where luminal electrolyte or non-electrolyte delivery from the medulla is altered, such as during salt-restriction or water deprivation. Finally, it is well known that changes in cell volume can produce a wide range of alterations in cell function including changes in protein synthesis and matrix synthesis (55, 110, 114). Therefore it is possible that macula densa cell volume may influence not only the functional properties of macula densa cells might also influence other elements within the juxtaglomerular apparatus.

Intracellular calcium studies

In previous work, photometry based fluorescence systems were utilized to assess $[NaCl]_L$-dependent changes in $[Ca^{2+}]_i$ from macula densa cells (81). The increases in $[Ca^{2+}]_i$ with elevations in $[NaCl]_L$ were at best modest. One disadvantage of this Ca^{2+} measuring system is that it involved placing a photometry window over the macula densa plaque and so it was not possible to glean information simultaneously from surrounding cells or other elements of the JGA. This limitation is resolved by the use of either wide-field or confocal imaging where information can be simultaneously obtained from a variety of structures from the JGA. In the present studies, the application of imaging technologies to assess $[Ca^{2+}]_i$ resulted in two significant findings. First, macula densa $[Ca^{2+}]_i$ was significantly lower compared to cTAL cells or other surrounding JGA structures. The reason for this finding is, at the present time, unclear. However, macula densa cells possess a unique cellular architecture displaying a very large nucleus and a cytoplasm that contains a large number of mitochondria. We speculate that macula densa cells may very efficiently buffer Ca^{2+}, perhaps due to the abundance of

mitochondria, and therefore maintain a lower level of $[Ca^{2+}]_i$. The validity of this idea will require future experimentation. The second finding of this study was the novel observation that certain tubular cells surrounding the macula densa plaque exhibited a pattern of Ca^{2+} oscillations. This observation led us to focus on the characterization of these oscillating cells as a potential new element in JGA signaling.

One reason that these oscillating tubular cells may be of interest in JGA signaling is based on ultrastructural studies by Barajas *et al.* which suggested that the intimate tubulo-vascular connection described originally at the macula densa extends beyond the borders of the macula densa plaque by ~ 100 μm. There is a close association between the cTAL, as it approaches the glomerulus, and the efferent arteriole. While Dorup *et al.* found a close anatomical association between the late distal/connecting tubular segment and afferent arteriole in rat superficial cortex (19). As shown in Figure 13, we observed that the region of contact between the tubular epithelium and the afferent arteriole, in rabbit, is not limited to the macula densa plaque: the afferent arteriole is positioned next the early distal tubule for ~ 100 μm. It should be noted that the initial post-macula densa tubular epithelium consists of the distal tubule and the connecting tubule. There appears to be some variability amongst nephrons and between species in terms of distance between transitions from one tubular segment to another.

To characterize Ca^{2+} oscillations in epithelial cells adjacent to the macula densa, we used wide-field ratiometric imaging with fura-2 as well as four-dimensional imaging using multiphoton confocal microscopy. The tubular epithelial cells in the perimeter of the macula densa before and after the glomerulus and on the opposite side of the macula densa demonstrated large spontaneous oscillations in $[Ca^{2+}]_i$. Similar to a recent study of reporting spontaneous $[Ca^{2+}]_i$ oscillations in isolated medullary thick ascending limbs (25), we were able to detect spontaneous $[Ca^{2+}]_i$ oscillations in the cTAL cells several hundred micrometers upstream from the macula densa. Interestingly a recent study has reported spontaneous oscillations in podocytes (78). The finding that cells in the perimeter of the macula densa also demonstrate spontaneous oscillations in membrane potential and that depolarization of the apical or basolateral membrane led to the cessation of $[Ca^{2+}]_i$ oscillations suggest that the generation of oscillations involves cyclic changes in membrane potential that drive depolarization-induced calcium entry.

This scenario is further supported by the fact that Ca^{2+} oscillations were dependent upon the presence of extracellular Ca^{2+}. However, for technical reasons we were not able to monitor $[Ca^{2+}]_i$ and membrane potential concurrently so, although it seems unlikely, we cannot exclude the possibility that $[Ca^{2+}]_i$ oscillations and membrane potential oscillations were occurring in different cells or that they were not associative.

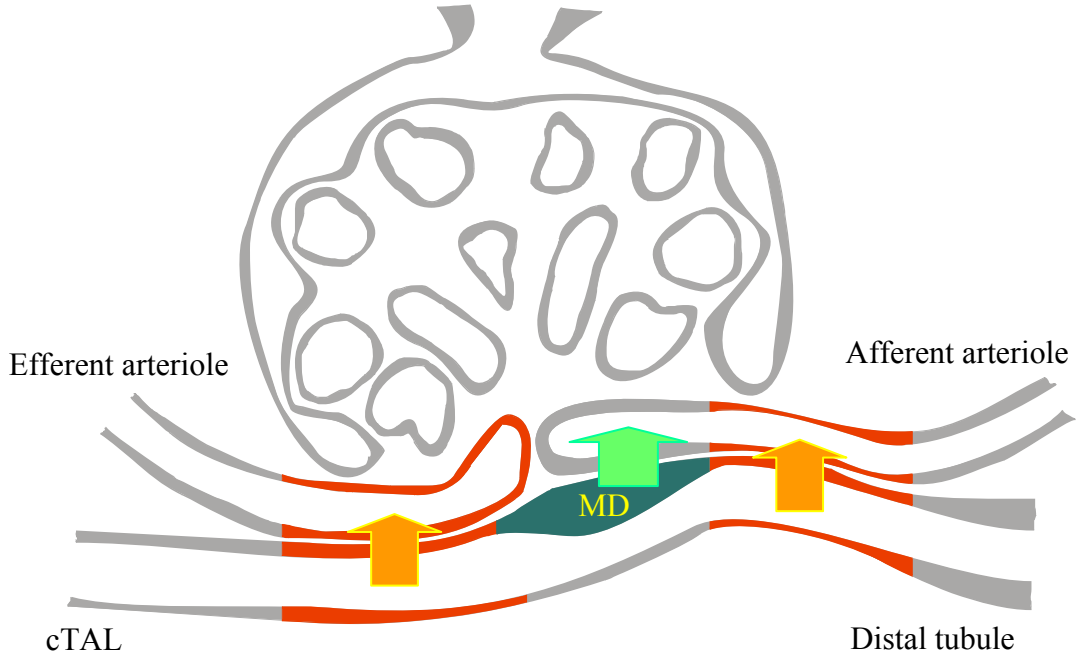

Figure 22 Schema for paramacular signaling.

The functional expression of calcium-sensing receptor has been implicated in the generation of oscillatory calcium signaling (10, 24). Immunohistochemical studies indicate a high level of expression of the calcium sensing receptor in renal tubules that are at or near the glomerular pole, including the macula densa segment (89). In the present studies we found that activation of the calcium-sensing receptor produced increases in Ca^{2+} oscillations and elevations in $[Ca^{2+}]_i$, and suggesting that calcium-sensing receptor contributes to Ca^{2+} signaling in the perimacular tubular cells.

Since increases in $[NaCl]_L$ have been implicated in the initiation of tubuloglomerular feedback responses, we investigated the effect of changes in luminal environment on $[Ca^{2+}]_i$ in perimacular cells. We have found that elevations in $[NaCl]_L$ resulted in marked increases in the amplitude of oscillations and increases in average

$[Ca^{2+}]_i$ in the perimacular oscillatory cells. Interestingly there was also an effect of luminal flow to increase the amplitude of Ca^{2+} oscillations in perimacular cells. This finding is consistent with recent studies that investigated the mechano-sensory function of apically located primary cilia. It has been shown that the bending of cilia that occurs in response to changes in luminal flow induce increases in $[Ca^{2+}]_i$ due, at least in part, to Ca^{2+} entry via polycystin-2 (71). All renal epithelial cells (with the possible exception of intercalated cells of the collecting duct) possess cilia and this is therefore consistent with the flow-dependent alterations in $[Ca^{2+}]_i$ in perimacular cells.

Finally we utilized four-dimensional imaging to assess overall signaling within the JGA and this information is presented in Figure 21. We observed that increases in $[NaCl]_L$ resulted in robust increases in $[Ca^{2+}]_i$ in the perimacular cells of the DT and in adjacent afferent arteriolar smooth muscle cells. There were also concomitant decreases in afferent arteriole diameter. There is precedent for non-macula densa mediated tubular to vascular signaling at the juxtaglomerular apparatus. Morsing *et al*. (69) reported and Ren *et al.* (87) recently confirmed that there is a feedback loop that involves the anatomical association of the latter part of the distal convoluted tubule which returns to and comes in contact with the afferent arteriole. This anatomical association is in addition to the tubulo-vascular contact that occurs adjacent to the glomerulus. Thus, there appears to be the potential for interactions between non-macula densa tubular segments and the vasculature.

We do not have direct evidence that the increases in DT $[Ca^{2+}]_i$ contributed to or were associated with the activation of afferent arteriole smooth muscle cell $[Ca^{2+}]_i$. However, these new finding are at least suggestive and should stimulate future research efforts in understanding communication processes between tubule and glomerular structures.

Conclusions

In summary, the present studies demonstrated several novel findings in the field of renal physiology. First, we have found that the signal that leads to the activation of tubuloglomerular signaling – elevations in tubular sodium delivery and osmolality – elicits macula densa shrinkage. Also, we have confirmed that the cells of the macula densa plaque are water permeable and have shown that they lack effective cell volume

regulation. We have shown that the macula densa cells have blunted intracellular cytosolic calcium signaling machinery, on the other hand, tubular epithelial cells in the vicinity of the plaque produce spontaneous oscillations in intracellular calcium concentration and basolateral membrane potential. In addition, these novel cells, termed perimacular cells, respond avidly to changes in luminal salt concentration, osmolality and tubular flow by elevations in intracellular calcium concentration, oscillatory amplitude or frequency. Interestingly, the oscillatory frequency of the intracellular calcium concentration in the perimacular cells coincides with the reported rhythm of the renal plasma flow and tubular fluid flow (37, 38, 39, 40, 122). Although, we have no evidence that the perimacular cells contribute to the regulation and timing of renal functioning, additional studies using *in vivo* techniques are needed to answer this question.

We have also found that there is an anatomical association of the early distal tubule segment (at the location of the perimacular cells) and the afferent arteriole. This is a novel finding and may prompt additional investigations seeking to explore the role of this association in the juxtaglomerular functioning. We have provided preliminary evidence that the activation of tubular epithelial intracellular calcium signaling in the perimacular cells leads to the activation of the afferent arteriolar smooth muscle cells and elicits vascular contraction. This non-macula densa-dependent tubulo-vasular communication represents a new paradigm in juxtaglomerular physiology.

Bibliography

1. Barajas L. (1979) Anatomy of the juxtaglomerular apparatus. Am J Physiol, 237: F333-F343.

2. Barajas L, Salido EC, Liu L, Powers KV. 1995. The juxtaglomerular apparatus: a morphologic perspective. In: Laragh JH, Brenner BM (szerk.) Hypertension: Pathophysiology, Diagnosis, and Management. Raven Press, Ltd., New York, 1995: 1335-1348.

3. Bell PD, Lapointe JY, Cardinal J. (1989) Direct measurement of basolateral membrane potentials from cells of the macula densa. Am J Physiol, 257: 463-8.

4. Bell PD, Lapointe JY, Peti-Peterdi J. (2003) Macula densa cell signaling. Annu Rev Physiol, 65: 481-500.

5. Bell PD, Lapointe JY, Sabirov R, Hayashi S, Peti-Peterdi J et al. (2003) Macula densa cell signaling involves ATP release through a maxi anion channel. Proc Natl Acad Sci U S A, 100: 4322-4327.

6. Bell PD, Navar LG. (1982) Cytoplasmic calcium in the mediation of macula densa tubulo-glomerular feedback responses. Science, 215: 670-3.

7. Bell PD, Peti-Peterdi J. (1999) Angiotensin II stimulates macula densa basolateral sodium/hydrogen exchange via type 1 angiotensin II receptors. J Am Soc Nephrol, 10 Suppl 11: S225-S229.

8. Bell PD, Reddington M. (1983) Intracellular calcium in the transmission of tubuloglomerular feedback signals. Am J Physiol, 245: F295-F302.

9. Boudreault F, Grygorczyk R. (2004) Cell swelling-induced ATP release is tightly dependent on intracellular calcium elevations. J Physiol, 561: 499-513.

10. Breitwieser GE, Gama L. (2001) Calcium-sensing receptor activation induces intracellular calcium oscillations. Am J Physiol Cell Physiol, 280: C1412-C1421.

11. Brown R, Ollerstam A, Johansson B, Skott O, Gebre-Medhin S et al. (2001) Abolished tubuloglomerular feedback and increased plasma renin in adenosine A1 receptor-deficient mice. Am J Physiol Regul Integr Comp Physiol, 281: R1362-R1367.

12. Burg MB, Green N. (1973) Function of the thick ascending limb of Henle's loop. Am J Physiol, 224: 659-668.

13. Burns DM, Stehno-Bittel L, Kawase T. (2004) Calcitonin gene-related peptide elevates calcium and polarizes membrane potential in MG-63 cells by both cAMP-independent and -dependent mechanisms. Am J Physiol Cell Physiol, 287: C457-C467.

14. Burnstock G. (1997) The Past, Present and Future of Purine Nucleotides as Signalling Molecules. Neuropharmacology, 36: 1127-1139.

15. Campean V, Theilig F, Paliege A, Breyer M, Bachmann S. (2003) Key enzymes for renal prostaglandin synthesis: site-specific expression in rodent kidney (rat, mouse). Am J Physiol Renal Physiol, 285: F19-F32.

16. Castrop H, Huang Y, Hashimoto S, Mizel D, Hansen P et al. (2004) Impairment of tubuloglomerular feedback regulation of GFR in ecto-5'-nucleotidase/CD73-deficient mice. J Clin Invest, 114: 634-642.

17. Christensen JA, Bohle A. (1978) The juxtaglomerular apparatus in the normal rat kidney. Virchows Arch A Pathol Anat Histol, 379: 143-150.

18. Clendenon JL, Phillips CL, Sandoval RM, Fang S, Dunn KW. (2002) Voxx: a PC-based, near real-time volume rendering system for biological microscopy. Am J Physiol Cell Physiol, 282: C213-C218.

19. Dorup J, Morsing P, Rasch R. (1992) Tubule-tubule and tubule-arteriole contacts in rat kidney distal nephrons. A morphologic study based on computer-assisted three-dimensional reconstructions. Lab Invest, 67: 761-769.

20. Drury AN, Szent-Gyorgyi A. (1929) The physiological activity of adenine compounds with special reference to their action upon the mammalian heart. J Physiol (Lond), 68: 213-237.

21. Foskett JK. 2000. Cell-volume control. In: Seldin DW, Giebisch G (szerk.) The Kidney Physiology & Pathophysiology. Lippincott Williams & Wilkins, Philadephia, 2000: 379-389.

22. Fowler BC, Chang YS, Laamarti A, Higdon M, Lapointe JY, Bell PD. (1995) Evidence for apical sodium proton exchange in macula densa cells. Kidney Int, 47: 746-751.

23. Fuson AL, Komlosi P, Unlap TM, Bell PD, Peti-Peterdi J. (2003) Immunolocalization of a microsomal prostaglandin E synthase in rabbit kidney. Am J Physiol Renal Physiol, 285: F558-F564.

24. Gerbino A, Ruder WC, Curci S, Pozzan T, Zaccolo M, Hofer AM. (2005) Termination of cAMP signals by Ca2+ and G(alpha)i via extracellular Ca2+ sensors: a link to intracellular Ca2+ oscillations. J Cell Biol, 171: 303-312.

25. Geyti CS, Odgaard E, Overgaard MT, Jensen ME, Leipziger J, Praetorius HA. (2007) Slow spontaneous [Ca(2+)] (i) oscillations reflect nucleotide release from renal epithelia. Pflugers Arch.

26. Golgi C. (1889) Annotazioni intorno all'istologia dei reni dell'uomo e di altri mammiferi e sull'istogenesi dei canalicoli oriniferi. Atti della Reale Accademia dei Lincei, 5: 334-342.

27. Gonzalez E, Salomonsson M, Muller-Suur C, Persson AE. (1988) Measurements of macula densa cell volume changes in isolated and perfused rabbit cortical thick ascending limb. I. Isosmotic and anisosmotic cell volume changes. Acta Physiol Scand, 133: 149-157.

28. Gonzalez E, Salomonsson M, Muller-Suur C, Persson AE. (1988) Measurements of macula densa cell volume changes in isolated and perfused rabbit cortical thick ascending limb. II. Apical and basolateral cell osmotic water permeabilities. Acta Physiol Scand, 133: 159-166.

29. Gorgas K. (1978) [Structure and innervation of the juxtaglomerular apparatus of the rat (author's transl)]. Adv Anat Embryol Cell Biol, 54: 3-83.

30. Gorren AC, Schrammel A, Schmidt K, Mayer B. (1998) Effects of pH on the structure and function of neuronal nitric oxide synthase. Biochem J, 331 (Pt 3): 801-807.

31. Grynkiewicz G, Poenie M, Tsien RY. (1985) A new generation of Ca2+ indicators with greatly improved fluorescence properties. J Biol Chem, 260: 3440-3450.

32. Gutierrez AM, Lou X, Erik A, Persson G, Ring A. (1999) Ca2+ response of rat mesangial cells to ATP analogues. Eur J Pharmacol, 369: 107-112.

33. Hanner F, Chambrey R, Bourgeois S, Meer E, Mucsi I et al. (2008) Increased renal renin content in mice lacking the Na+:H+ exchanger NHE2. Am J Physiol Renal Physiol.

34. Harris RC, McKanna JA, Akai Y, Jacobson HR, Dubois RN, Breyer MD. (1994) Cyclooxygenase-2 is associated with the macula densa of rat kidney and increases with salt restriction. J Clin Invest, 94: 2504-2510.

35. Harrison-Bernard LM, Navar LG, Ho MM, Vinson GP, el Dahr SS. (1997) Immunohistochemical localization of ANG II AT1 receptor in adult rat kidney using a monoclonal antibody. Am J Physiol, 273: F170-F177.

36. He XR, Greenberg SG, Briggs JP, Schnermann J. (1995) Effects of furosemide and verapamil on the NaCl dependency of macula densa-mediated renin secretion. Hypertension, 26: 137-142.

37. Holstein-Rathlou NH. (1991) A closed-loop analysis of the tubuloglomerular feedback mechanism. Am J Physiol, 261: F880-F889.

38. Holstein-Rathlou NH, Leyssac PP. (1986) TGF-mediated oscillations in the proximal intratubular pressure: differences between spontaneously hypertensive rats and Wistar-Kyoto rats. Acta Physiol Scand, 126: 333-339.

39. Holstein-Rathlou NH, Marsh DJ. (1989) Oscillations of tubular pressure, flow, and distal chloride concentration in rats. Am J Physiol, 256: F1007-F1014.

40. Holstein-Rathlou NH, Marsh DJ. (1994) Renal blood flow regulation and arterial pressure fluctuations: a case study in nonlinear dynamics. Physiol Rev, 74: 637-681.

41. Huang WC, Bell PD, Harvey D, Mitchell KD, Navar LG. (1988) Angiotensin influences on tubuloglomerular feedback mechanism in hypertensive rats. Kidney Int, 34: 631-637.

42. Hurst AM, Lapointe JY, Laamarti A, Bell PD. (1994) Basic properties and potential regulators of the apical K+ channel in macula densa cells. J Gen Physiol, 103: 1055-1070.

43. Inscho EW, Carmines PK, Navar LG. (1991) Juxtamedullary afferent arteriolar responses to P1 and P2 purinergic stimulation. Hypertension, 17: 1033-1037.

44. Inscho EW, Cook AK, Imig JD, Vial C, Evans RJ. (2003) Physiological role for P2X1 receptors in renal microvascular autoregulatory behavior. J Clin Invest, 112: 1895-1905.

45. Inscho EW, Cook AK, Mui V, Miller J. (1998) Direct assessment of renal microvascular responses to P2-purinoceptor agonists. Am J Physiol, 274: 718-27.

46. Inscho EW, Cook AK, Navar LG. (1996) Pressure-mediated vasoconstriction of juxtamedullary afferent arterioles involves P2-purinoceptor activation. Am J Physiol, 271: F1077-F1085.

47. Kaissling B, Kriz W. (1982) Variability of intercellular spaces between macula densa cells: a transmission electron microscopic study in rabbits and rats. Kidney Int Suppl, 12: S9-17.

48. Kirk KL, Bell PD, Barfuss DW, Ribadeneira M. (1985) Direct visualization of the isolated and perfused macula densa. Am J Physiol, 248: 890-4.

49. Kishore BK, Isaac J, Fausther M, Tripp SR, Shi H et al. (2005) Expression of NTPDase1 and NTPDase2 in murine kidney: relevance to regulation of P2 receptor signaling. Am J Physiol Renal Physiol, 288: F1032-F1043.

50. Komlosi P, Fintha A, Bell PD. (2006) Unraveling the relationship between macula densa cell volume and luminal solute concentration/osmolality. Kidney Int, 70: 865-871.

51. Komlosi P, Frische S, Fuson AL, Fintha A, Zsembery A et al. (2005) Characterization of basolateral chloride/bicarbonate exchange in macula densa cells. Am J Physiol Renal Physiol, 288: F380-F386.

52. Komlosi P, Peti-Peterdi J, Fuson AL, Fintha A, Rosivall L, Bell PD. (2004) Macula densa basolateral ATP release is regulated by luminal [NaCl] and dietary salt intake. Am J Physiol Renal Physiol, 286: F1054-F1058.

53. Kovacs G, Komlosi P, Fuson A, Peti-Peterdi J, Rosivall L, Bell PD. (2003) Neuronal nitric oxide synthase: its role and regulation in macula densa cells. J Am Soc Nephrol, 14: 2475-2483.

54. Kovacs G, Peti-Peterdi J, Rosivall L, Bell PD. (2002) Angiotensin II directly stimulates macula densa Na-2Cl-K cotransport via apical AT(1) receptors. Am J Physiol Renal Physiol, 282: F301-F306.

55. Lang F, Szabo I, Lepple-Wienhues A, Ritter M, Waldegger S, Gulbins E. 1998. Cell volume in the regulation of metabolism, cell proliferation and apoptotic cell death. In: Okada Y (szerk.) Cell Volume Regulation: The Molecular Mechanism and Volume Sensing Machinery. Elsevier Science B.V., Amsterdam, The Netherlands, 1998: 49-58.

56. Lapointe JY, Bell PD, Cardinal J. (1990) Direct evidence for apical Na+:2Cl-:K+ cotransport in macula densa cells. Am J Physiol, 258: F1466-F1469.

57. Lapointe JY, Bell PD, Hurst AM, Cardinal J. (1991) Basolateral ionic permeabilities of macula densa cells. Am J Physiol, 260: F856-F860.

58. Lapointe JY, Bell PD, Sabirov RZ, Okada Y. (2003) Calcium-activated nonselective cationic channel in macula densa cells. Am J Physiol Renal Physiol, 285: F275-F280.

59. Lapointe JY, Laamarti A, Bell PD. (1998) Ionic transport in macula densa cells. Kidney Int Suppl, 67: S58-S64.

60. Leipziger J. (2003) Control of epithelial transport via luminal P2 receptors. Am J Physiol Renal Physiol, 284: F419-F432.

61. Levine DZ, Iacovitti M, Burns KD, Zhang X. (2001) Real-time profiling of kidney tubular fluid nitric oxide concentrations in vivo. Am J Physiol Renal Physiol, 281: F189-F194.

62. Liu R, Carretero OA, Ren Y, Garvin JL. (2005) Increased intracellular pH at the macula densa activates nNOS during tubuloglomerular feedback. Kidney Int, 67: 1837-1843.

63. Liu R, Persson AE. (2005) Simultaneous changes of cell volume and cytosolic calcium concentration in macula densa cells caused by alterations of luminal NaCl concentration. J Physiol, 563: 895-901.

64. Liu R, Pittner J, Persson AE. (2002) Changes of cell volume and nitric oxide concentration in macula densa cells caused by changes in luminal NaCl concentration. J Am Soc Nephrol, 13: 2688-2696.

65. Lorenz JN, Weihprecht H, Schnermann J, Skott O, Briggs JP. (1991) Renin release from isolated juxtaglomerular apparatus depends on macula densa chloride transport. Am J Physiol, 260: F486-F493.

66. Majid DS, Inscho EW, Navar LG. (1999) P2 purinoceptor saturation by adenosine triphosphate impairs renal autoregulation in dogs. J Am Soc Nephrol, 10: 492-498.

67. Mitchell KD, Navar LG. (1988) Enhanced tubuloglomerular feedback during peritubular infusions of angiotensins I and II. Am J Physiol, 255: F383-F390.

68. Mitchell KD, Navar LG. (1993) Modulation of tubuloglomerular feedback responsiveness by extracellular ATP. Am J Physiol, 264: F458-F466.

69. Morsing P, Velazquez H, Ellison D, Wright FS. (1993) Resetting of tubuloglomerular feedback by interrupting early distal flow. Acta Physiol Scand, 148: 63-68.

70. Naruse M, Inoue T, Nakayama M, Sato T, Kurokawa K. (1994) Effect of luminal Cl- and Ca2+ on tubuloglomerular feedback mechanism. Jpn J Physiol, 44 Suppl 2: S269-S272.

71. Nauli SM, Alenghat FJ, Luo Y, Williams E, Vassilev P et al. (2003) Polycystins 1 and 2 mediate mechanosensation in the primary cilium of kidney cells. Nat Genet, 33: 129-137.

72. Navar LG, Lewis L, Hymel A, Braam B, Mitchell KD. (1994) Tubular fluid concentrations and kidney contents of angiotensins I and II in anesthetized rats. J Am Soc Nephrol, 5: 1153-1158.

73. Nicke A, Rettinger J, Schmalzing G. (2003) Monomeric and dimeric byproducts are the principal functional elements of higher order P2X1 concatamers. Mol Pharmacol, 63: 243-252.

74. Nishiyama A, Majid DS, Taher KA, Miyatake A, Navar LG. (2000) Relation between renal interstitial ATP concentrations and autoregulation-mediated changes in renal vascular resistance. Circ Res, 86: 656-662.

75. Nishiyama A, Majid DS, Walker M, III, Miyatake A, Navar LG. (2001) Renal interstitial atp responses to changes in arterial pressure during alterations in tubuloglomerular feedback activity. Hypertension, 37: 753-759.

76. Nishiyama A, Seth DM, Navar LG. (2002) Renal interstitial fluid concentrations of angiotensins I and II in anesthetized rats. Hypertension, 39: 129-134.

77. Okada SF, O'neal WK, Huang P, Nicholas RA, Ostrowski LE et al. (2004) Voltage-dependent Anion Channel-1 (VDAC-1) Contributes to ATP Release and Cell Volume Regulation in Murine Cells. J Gen Physiol, 124: 513-526.

78. Peti-Peterdi J. (2006) Calcium wave of tubuloglomerular feedback. Am J Physiol Renal Physiol, 291: F473-F480.

79. Peti-Peterdi J, Bebok Z, Lapointe JY, Bell PD. (2002) Novel regulation of cell [Na(+)] in macula densa cells: apical Na(+) recycling by H-K-ATPase. Am J Physiol Renal Physiol, 282: F324-F329.

80. Peti-Peterdi J, Bell PD. (1998) Regulation of macula densa Na:H exchange by angiotensin II. Kidney Int, 54: 2021-2028.

81. Peti-Peterdi J, Bell PD. (1999) Cytosolic [Ca2+] signaling pathway in macula densa cells. Am J Physiol, 277: F472-F476.

82. Peti-Peterdi J, Chambrey R, Bebok Z, Biemesderfer D, St John PL et al. (2000) Macula densa Na(+)/H(+) exchange activities mediated by apical NHE2 and basolateral NHE4 isoforms. Am J Physiol Renal Physiol, 278: F452-F463.

83. Peti-Peterdi J, Komlosi P, Fuson AL, Guan Y, Schneider A et al. (2003) Luminal NaCl delivery regulates basolateral PGE2 release from macula densa cells. J Clin Invest, 112: 76-82.

84. Peti-Peterdi J, Morishima S, Bell PD, Okada Y. (2002) Two-photon excitation fluorescence imaging of the living juxtaglomerular apparatus. Am J Physiol Renal Physiol, 283: F197-F201.

85. Prat AG, Reisin IL, Ausiello DA, Cantiello HF. (1996) Cellular ATP release by the cystic fibrosis transmembrane conductance regulator. Am J Physiol, 270: C538-C545.

86. Ren Y, Carretero OA, Garvin JL. (2002) Role of mesangial cells and gap junctions in tubuloglomerular feedback. Kidney Int, 62: 525-531.

87. Ren Y, Garvin JL, Liu R, Carretero OA. (2007) Crosstalk between the connecting tubule and the afferent arteriole regulates renal microcirculation. Kidney Int.

88. Reuss L. 2000. General principles of water transport. In: Seldin DW, Giebisch G (szerk.) The Kidney Physiology & Pathophysiology. Lippincott Williams & Wilkins, Philadephia, 2000: 321-340.

89. Riccardi D, Hall AE, Chattopadhyay N, Xu JZ, Brown EM, Hebert SC. (1998) Localization of the extracellular Ca2+/polyvalent cation-sensing protein in rat kidney. Am J Physiol, 274: F611-F622.

90. Rosivall L, MirzaHosseini S, Toma I, Sipos A, Peti-Peterdi J. (2006) Fluid flow in the juxtaglomerular interstitium visualized in vivo. Am J Physiol Renal Physiol, 291: F1241-F1247.

91. Rosivall L, Peti-Peterdi J, Razga Z, Fintha A, Bodor C, MirzaHosseini S. (2007) Renin-angiotensin system affects endothelial morphology and permeability of renal afferent arteriole. Acta Physiol Hung, 94: 7-17.

92. Rosivall L, Razga Z, Ormos J. (1991) Morphological characterization of human juxtaglomerular apparatus. Kidney Int Suppl, 32: S9-12.

93. Sabirov RZ, Dutta AK, Okada Y. (2001) Volume-dependent ATP-conductive large-conductance anion channel as a pathway for swelling-induced ATP release. J Gen Physiol, 118: 251-266.

94. Sabirov RZ, Okada Y. (2004) ATP-Conducting Maxi-Anion Channel: A New Player in Stress-Sensory Transduction. Jpn J Physiol, 54: 7-14.

95. Salomonsson M, Gonzalez E, Kornfeld M, Persson AE. (1993) The cytosolic chloride concentration in macula densa and cortical thick ascending limb cells. Acta Physiol Scand, 147: 305-313.

96. Salomonsson M, Gonzalez E, Sjolin L, Persson AE. (1990) Simultaneous measurement of cytosolic free Ca2+ in macula densa cells and in cortical thick

ascending limb cells using fluorescence digital imaging microscopy. Acta Physiol Scand, 138: 425-426.

97. Salomonsson M, Gonzalez E, Westerlund P, Persson AE. (1991) Intracellular cytosolic free calcium concentration in the macula densa and in ascending limb cells at different luminal concentrations of sodium chloride and with added furosemide. Acta Physiol Scand, 142: 283-290.

98. Schnermann J, Briggs J, Schubert G. (1982) In situ studies of the distal convoluted tubule in the rat. I. Evidence for NaCl secretion. Am J Physiol, 243: F160-F166.

99. Schnermann J, Briggs JP. (1990) Restoration of tubuloglomerular feedback in volume-expanded rats by angiotensin II. Am J Physiol, 259: F565-F572.

100. Schnermann J, Briggs JP. 2000. Function of the juxtaglomerular apparatus: control of glomerular hemodynamics and renin secretion. In: Seldin DW, Giebisch G (szerk.) The Kidney Physiology & Pathophysiology. Lippincott Williams & Wilkins, Philadephia, 2000: 945-980.

101. Schnermann J, Levine DZ. (2003) Paracrine factors in tubuloglomerular feedback: adenosine, ATP, and nitric oxide. Annu Rev Physiol, 65: 501-529.

102. Schnermann J, Marver D. (1986) ATPase activity in macula densa cells of the rabbit kidney. Pflugers Arch, 407: 82-86.

103. Schnermann J, Weihprecht H, Briggs JP. (1990) Inhibition of tubuloglomerular feedback during adenosine1 receptor blockade. Am J Physiol, 258: F553-F561.

104. Schnermann JB, Traynor T, Yang T, Huang YG, Oliverio MI et al. (1997) Absence of tubuloglomerular feedback responses in AT1A receptor-deficient mice. Am J Physiol, 273: F315-F320.

105. Schwiebert EM, Zsembery A. (2003) Extracellular ATP as a signaling molecule for epithelial cells. Biochim Biophys Acta, 1615: 7-32.

106. Sun D, Samuelson LC, Yang T, Huang Y, Paliege A et al. (2001) Mediation of tubuloglomerular feedback by adenosine: evidence from mice lacking adenosine 1 receptors. Proc Natl Acad Sci U S A, 98: 9983-9988.

107. Suzuki M, Mizuno A. (2004) A novel human Cl(-) channel family related to Drosophila flightless locus. J Biol Chem, 279: 22461-22468.

108. Taylor AL, Kudlow BA, Marrs KL, Gruenert DC, Guggino WB, Schwiebert EM. (1998) Bioluminescence detection of ATP release mechanisms in epithelia. Am J Physiol, 275: C1391-C1406.

109. Thomson S, Bao D, Deng A, Vallon V. (2000) Adenosine formed by 5'-nucleotidase mediates tubuloglomerular feedback. J Clin Invest, 106: 289-298.

110. Tilly BC, van der Wijk T, de Jonge HR. 1998. Activation of cellular signalling pathways by hypotonicity. In: Okada Y (szerk.) Cell Volume Regulation: The Molecular Mechanism and Volume Sensing Machinery. Elsevier Science B.V., Amsterdam, The Netherlands, 1998: 59-66.

111. Turner CM, Vonend O, Chan C, Burnstock G, Unwin RJ. (2003) The pattern of distribution of selected ATP-sensitive P2 receptor subtypes in normal rat kidney: an immunohistological study. Cells Tissues Organs, 175: 105-117.

112. Uhlen P. (2004) Spectral analysis of calcium oscillations. Sci STKE, 2004: l15.

113. Unwin RJ, Bailey MA, Burnstock G. (2003) Purinergic signaling along the renal tubule: the current state of play. News Physiol Sci, 18: 237-241.

114. Waldegger S, Lang F. (1998) Cell volume-regulated gene transcription. Kidney Blood Press Res, 21: 241-244.

115. Wang H, Carretero OA, Garvin JL. (2003) Inhibition of apical Na+/H+ exchangers on the macula densa cells augments tubuloglomerular feedback. Hypertension, 41: 688-691.

116. Wang H, Garvin JL, Carretero OA. (2001) Angiotensin II enhances tubuloglomerular feedback via luminal AT(1) receptors on the macula densa. Kidney Int, 60: 1851-1857.

117. Wilcox CS, Welch WJ, Murad F, Gross SS, Taylor G et al. (1992) Nitric oxide synthase in macula densa regulates glomerular capillary pressure. Proc Natl Acad Sci U S A, 89: 11993-11997.

118. Wright FS, Schnermann J. (1974) Interference with feedback control of glomerular filtration rate by furosemide, triflocin, and cyanide. J Clin Invest, 53: 1695-1708.

119. Xu JZ, Hall AE, Peterson LN, Bienkowski MJ, Eessalu TE, Hebert SC. (1997) Localization of the ROMK protein on apical membranes of rat kidney nephron segments. Am J Physiol, 273: F739-F748.

120. Yang T, Huang YG, Singh I, Schnermann J, Briggs JP. (1996) Localization of bumetanide- and thiazide-sensitive Na-K-Cl cotransporters along the rat nephron. Am J Physiol, 271: F931-F939.

121. Yang T, Park JM, Arend L, Huang Y, Topaloglu R et al. (2000) Low chloride stimulation of prostaglandin E2 release and cyclooxygenase-2 expression in a mouse macula densa cell line. J Biol Chem, 275: 37922-37929.

122. Yip KP, Holstein-Rathlou NH, Marsh DJ. (1993) Mechanisms of temporal variation in single-nephron blood flow in rats. Am J Physiol, 264: F427-F434.

123. Zimmermann H. (2000) Extracellular metabolism of ATP and other nucleotides. Naunyn Schmiedebergs Arch Pharmacol, 362: 299-309.

Bibliography of the candidate's publications

1. Banizs B, Pike MM, Millican CL, Ferguson WB, Komlosi P et al. (2005) Dysfunctional cilia lead to altered ependyma and choroid plexus function, and result in the formation of hydrocephalus. Development, 132: 5329-5339.

2. Banizs B, Komlosi P, Bevensee MO, Schwiebert EM, Bell PD, Yoder BK. (2007) Altered pH(i) regulation and Na(+)/HCO3(-) transporter activity in choroid plexus of cilia-defective Tg737(orpk) mutant mouse. Am J Physiol Cell Physiol, 292: C1409-C1416.

3. Fuson AL, Komlosi P, Unlap TM, Bell PD, Peti-Peterdi J. (2003) Immunolocalization of a microsomal prostaglandin E synthase in rabbit kidney. Am J Physiol Renal Physiol, 285: F558-F564.

4. Komlosi P, Fuson AL, Fintha A, Peti-Peterdi J, Rosivall L et al. (2003) Angiotensin I conversion to angiotensin II stimulates cortical collecting duct sodium transport. Hypertension, 42: 195-199.

5. Komlosi P, Peti-Peterdi J, Fuson AL, Fintha A, Rosivall L, Bell PD. (2004) Macula densa basolateral ATP release is regulated by luminal [NaCl] and dietary salt intake. Am J Physiol Renal Physiol, 286: F1054-F1058.

6. Komlosi P, Fintha A, Bell PD. (2004) Current mechanisms of macula densa cell signalling. Acta Physiol Scand, 181: 463-469.

7. Komlosi P, Frische S, Fuson AL, Fintha A, Zsembery A et al. (2005) Characterization of basolateral chloride/bicarbonate exchange in macula densa cells. Am J Physiol Renal Physiol, 288: F380-F386.

8. Komlosi P, Fintha A, Bell PD. (2005) Renal cell-to-cell communication via extracellular ATP. Physiology (Bethesda), 20: 86-90.

9. Komlosi P, Fintha A, Bell PD. (2006) Unraveling the relationship between macula densa cell volume and luminal solute concentration/osmolality. Kidney Int, 70: 865-871.

10. Kovacs G, Komlosi P, Fuson A, Peti-Peterdi J, Rosivall L, Bell PD. (2003) Neuronal nitric oxide synthase: its role and regulation in macula densa cells. J Am Soc Nephrol, 14: 2475-2483.

11. Kovacs GG, Zsembery A, Anderson SJ, Komlosi P, Gillespie GY et al. (2005) Changes in intracellular Ca2+ and pH in response to thapsigargin in human glioblastoma cells and normal astrocytes. Am J Physiol Cell Physiol, 289: C361-C371.

12. Peti-Peterdi J, Komlosi P, Fuson AL, Guan Y, Schneider A et al. (2003) Luminal NaCl delivery regulates basolateral PGE2 release from macula densa cells. J Clin Invest, 112: 76-82.

13. Siroky BJ, Ferguson WB, Fuson AL, Xie Y, Fintha A et al. (2006) Loss of primary cilia results in deregulated and unabated apical calcium entry in ARPKD collecting duct cells. Am J Physiol Renal Physiol, 290: F1320-F1328.

14. Unlap MT, Bates E, Williams C, Komlosi P, Williams I et al. (2003) Na+/Ca2+ exchanger: target for oxidative stress in salt-sensitive hypertension. Hypertension, 42: 363-368.

15. Unlap MT, Williams C, Morin D, Siroky B, Fintha A et al. (2005) Amyloid beta peptide 1-40 stimulates the Na+/Ca2+ exchange activity of SNCX. Curr Neurovasc Res, 2: 3-12.

Acknowledgements

I would like to thank:

Dr. Darwin Bell, Professor and Head of the Renal Biology Laboratory at the Medical University of South Carolina, my mentor, who helped and supported my research work with great enthusiasm.

Dr. János Peti-Peterdi, Associate Professor, University of South California, who introduced me to a lot of scientific techniques used in the present studies.

I would like to thank **Dr. László Rosivall**, Professor of Pathophysiology, Nephrology Research and Training Center, Institute of Pathophysiology, Faculty of Medicine, Semmelweis University, Budapest, Ph.D. program director, for helping me continuously along my career. .

I am grateful to **Dr. Miklós Molnár**, Institute of Pathophysiology, Faculty of Medicine, Semmelweis University, for introducing research during my student researcher years.

I would like to thank **Dr. Gergely Kovács and Dr. Attila Fintha** for a lot of helpful discussion about our research.

I would like to thank my collegaues at the Institute of Pathophysiology, Semmelweis University and at the Medical University of South Carolina and the University of Alabama at Birmingham for their help and the friendly atmosphere.

I dedicate my work to Bogi, Mom and Dad, my sons, Gergely and Dániel.

Abstract

The juxtaglomerular apparatus plays an important role in the regulation of renal hemodynamics and in the control of renin release. Elevations in distal tubular salt delivery are sensed by the tubular epithelium (including the macula densa) which leads to the constriction of the adjacent afferent arteriole. In the present studies we utilized the isolated double perfused afferent arteriole-glomerular preparation with attached cortical thick ascending limb. To study changes in cell volume and the intracellular calcium concentration, basolateral membrane potential, we used multiphoton fluorescence microscopy and fluorescent dyes calcein, fluo-4, $DiBAC_4(3)$, respectively. We concluded that concomitant elevations in luminal sodium chloride concentration and osmolality produce macula densa cell shrinkage. This change in cell volume is maintained, suggesting the cells' limited ability to regulate their cell volume. The intracellular calcium concentration in the macula densa cells is relatively low and unresponsive to physiological challenges in the tubular lumen. On the other hand, cells in the vicinity of the plaque, called perimacular cells produce spontaneous oscillations in intracellular calcium concentration and basolateral membrane potential and produce characteristic changes in the pattern of intracellular calcium signaling. The early distal tubule and the adjacent afferent arteriole establish a close anatomical region of contact and functional relationship, suggesting that the perimacular cells and the connection of the early distal tubule and the afferent arteriole contribute to the paracrine signaling machinery of the juxtaglomerular apparatus.

Abstract in Hungarian (Összefoglalás)

A juxtaglomaruláris apparátus részt vesz a vese véráramlásának szabályozásában, valamint a renin hormon termelésében. A tubuláris sókoncentráció emelkedését a tubulus hámsejtek (köztük a macula densa sejtek) érzékelik, s ez vazokonstrikciót okoz a szomszédos afferens artriolában. Jelen vizsgálatainkban izolált és perfundált afferens arteriolákat és vesetestecskéket valamint a hozzájuk kapcsolt felszálló vastag szegmenetumot használtuk. A sejtek intracelluláris jelátvitelének tanulmányozásához multifoton fluoreszcens mikroszkópiát használtunk. Megállapítottuk, hogy a macula densa sejtek térfogata csökken fiziológiás sóterhelés hatására. Ezen sejttérfogat-változás fennmarad, míg az tubuláris sókoncentráció megemelkedett, jelezve hogy ezen sejtek vízpermeabilitása magas, valamint azon képességük, hogy korrigálják a primer térfogatváltozást, korlátozott. Kimutattuk, hogy a macula densa sejtek intracelluláris kalcium koncentrációja alacsonyabb a környező sejtekben mérhetőnél, a macula densa plakk körüli sejtekben az intracelluláris kalcium koncentráció és a bazolaterális transzmembrán potenciál spontán oszcillációkat mutat. Ezen „perimakuláris" sejtekben a tubuláris folyadék sókoncentrációjának, osmolalitásának és áramlási sebességének változásai specifikus változásokat indukálnak a intracelluláris kalcium homeosztázisban. Megfigyeltük, hogy a disztális tubulus első szakasza, valamint az afferens artriola szoros anatómiai és funkcionális kapcsolatot létesít, s így ezek a sejtek is szerepet játszhatnak a juxtaglomeruláris apparátus működésében.